A study of ozone depletion in the 2004/2005 Arctic winter based on data from Odin/SMR and Aura/MLS

J. D. Rösevall,[1] D. P. Murtagh,[1] J. Urban,[1] W. Feng,[2] P. Eriksson,[1] and S. Brohede[1]

[1]   Ozone depletion in the colder than average 2004/2005 Arctic polar vortex is mapped and quantified using ozone profiles from two limb sounding satellite instruments, the Earth Observing System Microwave Limb Sounder (Aura/MLS) and the Odin Sub-Millimetre Radiometer (Odin/SMR). Profiles of chemically inert nitrous oxide (N_2O) are used to trace vertical transport during the winter. Two methods are used for estimating the vortex average ozone losses north of $67°$ equivalent latitude. In a first step, the time evolution of ozone mixing ratios is described on N_2O isopleths. Maximum ozone depletion is found on the 100 ppbv and 150 ppbv N_2O isopleths (located in the $430-460$ K potential temperature range in mid-March 2005) where vortex average ozone depletion totalled $1.0-1.1$ ppmv for Aura/MLS and $0.7-0.9$ ppmv for Odin/SMR. Second, ozone profiles from Aura/MLS and Odin/SMR are assimilated into the DIAMOND isentropic transport model. Ozone depletion is estimated by comparing assimilated fields to ozone fields passively transported from 1 January. On the 450 K potential temperature level, the Aura/MLS ozone fields indicate $0.9-1.3$ ppmv vortex-averaged ozone depletion while the Odin/SMR fields indicate $0.6-0.9$ ppmv depletion. The uncertainty depends mainly on the rates of cross-isentropic transport used in the study. The ozone depletion estimates in this study are lower than previously published estimates. The discrepancies to some studies can be attributed to the more adequate treatment of an ozone poor region that is found in the central polar vortex in the early winter.

Citation: Rösevall, J. D., D. P. Murtagh, J. Urban, W. Feng, P. Eriksson, and S. Brohede (2008), A study of ozone depletion in the 2004/2005 Arctic winter based on data from Odin/SMR and Aura/MLS, *J. Geophys. Res.*, *113*, D13301, doi:10.1029/2007JD009560.

1. Introduction

[2]   Heterogenous ozone destruction in the Arctic polar vortex exhibits large inter annual variations. Large-scale destruction of ozone has been observed after winters with vortex temperatures low enough to sustain polar stratospheric clouds while little destruction of ozone can be seen after warmer winters [*Tilmes et al.*, 2004]. The unusually cold Arctic polar vortex of 2004/2005 had temperatures low enough to sustain polar stratospheric clouds from mid-December to early March [e.g., *Feng et al.*, 2007; *Singleton et al.*, 2007], which led to substantial chlorine activation [e.g., *Urban et al.*, 2006; *von Hobe et al.*, 2006; *Tilmes et al.*, 2006a]. Strong planetary wave activity in February and March [*Manney et al.*, 2006] however led to intrusions of extravortex air. This did not necessarily reduce chemical ozone loss but likely masked the signature of ozone depletion in sonde and satellite measurements of vortex ozone. Furthermore, the vortex broke up in mid-March which limited the further destruction of ozone.

[3]   Several studies report severe ozone destruction in the 2004/2005 Arctic winter. On the basis of vortex average analysis of O_3 and N_2O data from the Microwave Limb Sounder on board the Aura satellite (Aura/MLS), *Manney et al.* [2006] estimate $1.2-1.5$ ppmv vortex-averaged ozone loss between 5 January and 10 March in the 450 K to 500 K potential temperature range, with up to $\sim$2 ppmv loss in the outer vortex near 500 K. In another study using vortex average as well as tracer correlation analysis of data from the Fourier Transform Spectrometer (FTS) instrument on board the Atmospheric Chemistry Experiment (ACE) satellite, *Jin et al.* [2006] on the other hand estimate $\sim$2.1 ppmv mixing ratio losses in the 450 K to 500 K range between the first 7 days of January and $8-15$ March. Vortex-averaged ozone losses of $1.3-2.1$ ppmv on the 450 K level and $0.7-1.6$ ppmv on the 500 K level between 5 January and 25 March are furthermore presented in a study by *Rex et al.* [2006] that is based on the Match technique [*Rex et al.*, 1999] and data from in situ sondes. *Rex et al.* [2006] also reached similar

---

[1]Department of Radio and Space Science, Chalmers University of Technology, Göteborg, Sweden.
[2]Institute for Atmospheric Science, School of Earth and Environment, University of Leeds, Leeds, UK.

results using a vortex average descent approach [*Hoppel et al.*, 2002] with data from the SAGE III and POAM III satellite instruments.

[4] On potential temperature levels below ∼500 K, ozone mixing ratios inside the polar vortex are generally higher than in the extra vortex air. Intrusions of extra vortex air masses into the polar vortex thus lead to lower ozone mixing ratios in the lower vortex. The N_2O mixing ratios in extra vortex air are however significantly higher than the N_2O mixing ratios found inside the vortex. Hence intrusions of extra vortex air can actually lead to underestimation of ozone losses in studies based on ozone-N_2O correlation [*Müller et al.*, 2005]. The difficulty of separating chemical ozone depletion from cross vortex transport is discussed by *Manney et al.* [2006] and *Jin et al.* [2006]. Both suggest transport model simulations of the Arctic vortex as a possible method for overcoming the problem.

[5] *Singleton et al.* [2007] estimate ozone depletion in the 2004/2005 Arctic vortex by comparing a passive ozone tracer field from the SLIMCAT chemical transport model [*Chipperfield*, 2005], to ozone measurements from various satellite instruments (POAM III, SAGE III, Aura/MLS, ACE/FTS, ACE/MAESTRO). The passive transport is started on 1 December 2004 and the initial ozone tracer field is obtained by running the SLIMCAT model with full chemistry for several years until that date. By mid-March 2005, the study indicates 1.8–2.3 ppmv vortex average ozone depletion in the 425 K to 500 K potential temperature range.

[6] In this study, the DIAMOND transport and assimilation model [*Rösevall et al.*, 2007], has been used in a similar way with ozone data retrieved by the Odin/SMR and Aura/MLS satellite instruments. The passive transport is however started on 1 January 2005 since *Singleton et al.* [2007] found less than 0.2 ppmv ozone depletion in December 2004. Initial tracer fields are obtained by assimilating Odin/SMR or Aura/MLS ozone data from August 2004 until 31 December 2004. Obtaining the initial tracer fields by data assimilation avoids having biases between the passive ozone tracer fields and the satellite data at the start of passive transport.

[7] The rates and geographical distribution of polar ozone depletion are mapped by comparing the passive ozone tracer fields to DIAMOND model fields in which satellite data have been assimilated after 1 January. For comparison, the ozone depletion in the 2004/2005 Arctic vortex is also studied using a vortex descent method in which the correlation of ozone to the chemically inert tracer N_2O has been used to compensate for cross-isentropic transport. Both methods infer less ozone depletion than estimated in the earlier studies described above.

[8] The Odin/SMR and Aura/MLS satellite instruments are described in section 2 of this article and the DIAMOND transport and assimilation model is described in section 3. A short description of the 2004/2005 Arctic winter including a study of vertical and horizontal transport processes in the 2004/2005 Arctic polar vortex are presented in section 4 and a model study of cross-isentropic transport is presented in section 5. Estimates of vortex average ozone depletion by the vortex descent method are given in section 6 while a model study of ozone depletion is presented in section 7. A summary of our results and a detailed discussion of the discrepancies between our ozone depletion estimates and

the results presented by *Manney et al.* [2006], *Jin et al.* [2006], *Rex et al.* [2006] and *Singleton et al.* [2007] are given in section 8.

2. Satellite Data

2.1. Odin/SMR Data

[9] Odin is a Swedish-led satellite mission designated for radio astronomy and limb sounding of the Earth middle atmosphere [*Murtagh et al.*, 2002]. Measurement time is equally shared between the two disciplines meaning that ∼50% of the satellite's operational time is used for aeronomy. The satellite completes ∼15 near-terminator polar orbits per day with descending and ascending nodes at 0600 and 1800 local solar time respectively. Its payload comprises two different limb sounding instruments, OSIRIS (Optical Spectrograph/Infrared Imaging System) and SMR (Sub-Millimetre Radiometer).

[10] The SMR instrument [*Frisk et al.*, 2003] comprises four tunable Schottky-diode single-sideband heterodyne microwave receivers. In the basic mode for stratospheric observations, two of the receivers, covering the 486–504 and 541–558 GHz frequency bands respectively, are used for detecting microwave emission lines in the spectra of O_3, N_2O, ClO and HNO_3. On average, 1 day out of 3 is dedicated to this mode. Odin/SMR measurements of stratospheric ozone and N_2O are thus normally only available for one 24 h period every third day.

[11] The ozone data used in this study have been retrieved from an emission line at 501.5 GHz using the Chalmers-v2.1 retrieval scheme. The main difference between this version of the retrieval scheme compared to version 2.0, described in *Urban et al.* [2006], is a better separation of target line and out-of-band contributions to the spectra by the retrieval algorithm. All ozone profiles used in this study have "quality" flag equal to zero. We also require the measurement response to be higher than 70%.

[12] The Odin/SMR ozone profiles cover the altitude range ∼17–50 km with an altitude resolution of 2.5–3.5 km and an estimated single-profile precision of ∼1.5 ppmv [*Urban et al.*, 2006]. In this study we do not use Odin/SMR data to study ozone depletion at altitudes below 450 K potential temperature (∼19 km in the polar vortex) since the measurement response is generally below 70% at lower altitudes. Systematic differences between Odin/SMR v2.1 ozone data and balloon sonde measurements have been studied in detail by *Jones et al.* [2007]. The investigation shows that Odin/SMR ozone profiles in the 60–90°N latitude band have a positive bias of 0.1–0.3 ppmv in the 23 to 30 km altitude range while Odin/SMR ozone mixing ratios are 0.0–0.1 ppmv lower than sonde measurements below 23 km. Since air masses descend during winter the dependence of the systematic errors on altitude is one possible source of error when comparing ozone mixing ratios in early winter to ozone mixing ratios in spring.

[13] Odin/SMR N_2O profiles used in this study have been retrieved using the Chalmers-v2.1 retrieval scheme from an emission line at 502.3 GHz. The profiles cover altitudes in the range 12–60 km with an altitude resolution of ∼1.5 km. The estimated single-profile precision is ∼30 ppbv while the magnitude of systematic errors in the data are estimated to be

less than 12 ppbv [*Urban et al.*, 2006]. All N_2O profiles used in this study have "quality" flag equal to zero and measurement response is required to be higher than 70%.

2.2. Aura/MLS Data

[14] The Earth Observing System (EOS) Microwave Limb Sounder (MLS) is one of four instruments on board the Aura satellite launched on 15 July 2004. The mission objective of Aura is to monitor the Earth's climate, ozone layer and air quality. The satellite completes 13 near-polar orbits per day with descending and ascending nodes around 0745 and 1345 local solar time [*Schoeberl et al.*, 2006].

[15] The MLS instrument [*Waters et al.*, 2006] measures thermal emission from five spectral bands centered near 118, 190, 240, 640 and 2250 GHz using 7 microwave receivers. Atmospheric profiles for more than a dozen trace species can be retrieved from the spectra. In this study we use ozone and N_2O profiles that are retrieved from emission lines in the 240 GHz and 640 GHz bands respectively, using Aura/MLS retrieval scheme version 1.5 [*Livesey et al.*, 2006]. In accordance with the recommendations by *Livesey et al.* [2005] we do not use ozone profiles with "quality" flag below 0.1 or N_2O profiles with "quality" flag below 2.5. Profiles with negative precision values are also discarded. *Livesey et al.* [2005] furthermore show that the Aura/MLS version 1.5 retrieval scheme occasionally produces high biased N_2O mixing ratios in the polar vortex and near-vortex regions. Such N_2O profiles have been screened out using data flags obtained from N. J. Livesey (private communications, 2007).

[16] The altitude resolution of the ozone profiles is ~3 km in the lower stratosphere and the single-profile precision reported by the Level 2 software typically varies between 0.2 and 0.4 ppmv. A study by *Froidevaux et al.* [2006] however indicates that the real precision standard deviation of the Aura/MLS ozone profiles is 30% to 100% larger. In the same study, Aura/MLS ozone profiles in the lower stratosphere are furthermore described as having mixing ratios that are somewhere around 0–10% below balloon sonde measurements.

[17] The altitude resolution of the N_2O profiles is 4–5 km and the single-profile precision in the lower stratosphere is below 30 ppbv. Comparison of Aura/MLS N_2O profiles to balloon sondes furthermore indicates that systematic errors in the satellite profiles are less than 15 ppbv [*Froidevaux et al.*, 2006].

[18] Since this article was first submitted for review, a new version of Aura/MLS inversions have been released (version 2.2). We do not use it in this study since v2.2 data for the 2004/2005 winter are only recently processed. The new version of N_2O profiles are however compared to Odin/SMR N_2O profiles in a study by *Lambert et al.* [2007]. The study indicates that v2.2 Aura/MLS N_2O mixing ratios are 0–20 ppbv below coincident Odin/SMR N_2O mixing ratios in the pressure range 50–100 hPa with stronger bias at higher pressure levels. N_2O mixing ratios in the v1.5 Aura/MLS data product used in this study are however systematically 0–30 ppbv higher than version 2.2 in the 50–100 hPa range, also with stronger bias at higher pressure levels. Thus we expect Aura/MLS version 1.5 N_2O mixing ratios to agree or have a positive bias compared to Odin/SMR version 2.1 N_2O in the lowermost stratosphere. Aura/

MLS and Odin/SMR N_2O mixing ratios in the 2004/2005 Arctic polar vortex are however compared in section 5 of this study. We conclude that Aura/MLS N_2O mixing ratios in the polar vortex are in fact ~20 ppbv below the Odin/SMR mixing ratios until late February when the Aura/MLS N_2O mixing ratios rise to the levels measured by Odin/SMR. The vertical gradients of Aura/MLS and Odin/SMR N_2O agree well in the early winter while Aura/MLS N_2O mixing ratios drop more rapidly as a function of altitude after late February.

3. DIAMOND Model

[19] The DIAMOND model [*Rösevall et al.*, 2007] is an off-line wind-driven transport and assimilation model designed to simulate ozone transport in the lower stratosphere with low numerical diffusivity. In this study the model is used for estimating loss of ozone by comparing assimilated tracer fields to passively transported fields initialized by assimilation. Chemistry is omitted from the model since it could force the tracer fields away from the pure satellite measurements.

[20] Wind-driven advection in the horizontal plane is implemented using the low-diffusive transport scheme of *Prather* [1986]. The transport scheme is forced by wind fields from the European Centre for Medium-Range Weather Forecasts (ECMWF). Horizontal advection is implemented on separate isentropic surfaces (i.e., surfaces with constant potential temperature) spaced at 25 K intervals between 400 K and 1000 K. It should however be noted that the intrinsic vertical resolutions of Odin/SMR and Aura/MLS profiles are rather of the order 50 K.

[21] Satellite data are assimilated into the transport model using a sequential algorithm that can be described as a variant of the Kalman filter. Fields containing estimates of the errors in the model are thus built up and transported alongside the tracer fields for the purpose of weighting in new data in an optimal way. A detailed description of the approach used is given by *Rösevall et al.* [2007].

[22] In this study Odin/SMR and Aura/MLS ozone profiles have been assimilated in separate runs of the 2004/2005 Arctic winter. The assimilated fields have been validated by comparison to ECC type ozonesondes [*Komhyr and Harris*, 1971] that have accuracy of order ±(4–5)% and precision within ±(3–4)% in the lower and middle stratosphere [*Smit and Kley*, 1996]. Comparison of assimilated fields to sonde measurements made at Ny-Ålesund on Svalbard (78°55 N, 11°56 E) and at Payerne Switzerland (46°82 N, 6°95 E) are presented in Figures 1 and 2, respectively. The solid lines represent the ozone mixing ratios in the model directly above the sonde stations and the dots represent ozonesonde measurements. During Arctic winters, sondes from the Ny-Ålesund station normally probe air masses inside the polar vortex while sondes from the Payerne station primarily probe air masses located outside it.

[23] Agreement between sondes and assimilated Odin/SMR ozone can be seen on and above the 450 K level. Below 450 K, Odin/SMR 501.5 GHz ozone retrievals do not contain enough measurement information to accurately describe the ozone layer. The average difference between sondes and assimilated Odin/SMR ozone is below 0.16 ppmv and the standard deviation is ~0.3 ppmv. Agreement between
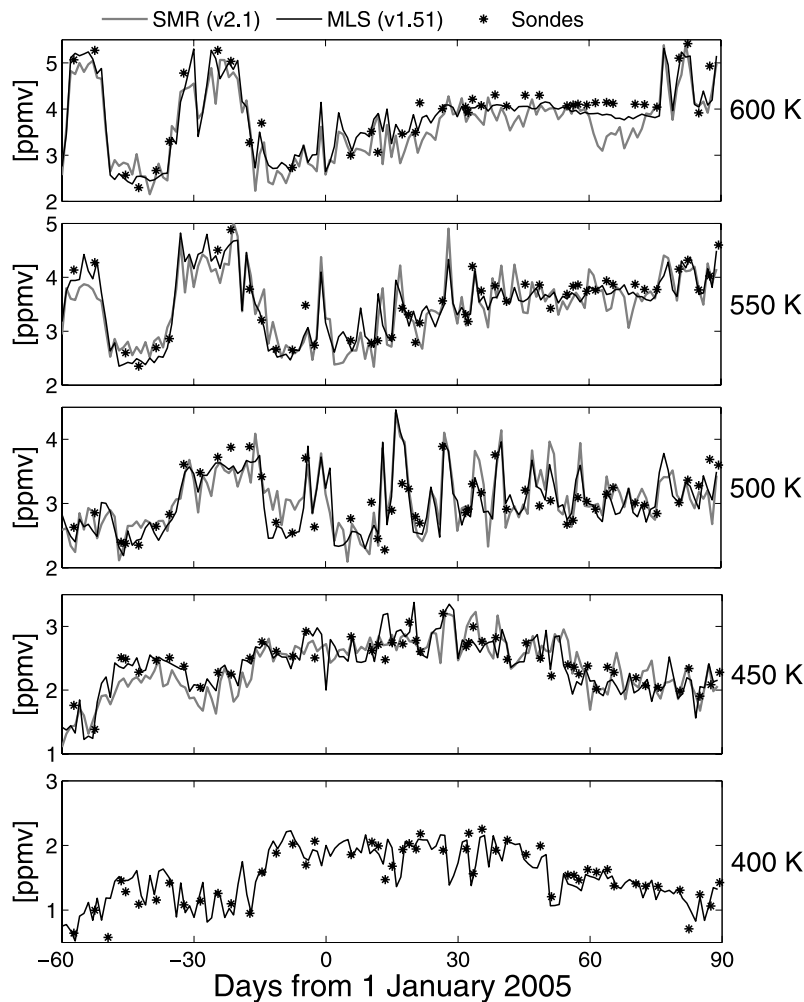
Figure 1. Comparison of ozonesondes released from Ny-Å lesund on Svalbard (78°55 N, 11°56 E) to assimilated fields of Aura/MLS (v1.51) and Odin/SMR (501.5 GHz, v2.1) ozone. The solid lines represent the ozone mixing ratios directly above Ny-Å lesund in the DIAMOND model, and the dots represent ozonesonde measurements. Odin/SMR ozone is not shown on the 400 K level (see the text for details).

sondes and assimilated fields of Aura/MLS data can be seen on all levels with less than 0.10 ppmv average difference and a standard deviation of ∼0.2 ppmv.

[24] In the Northern Hemisphere, planetary wave activity causes filamentation of the stratosphere which leads to sharp horizontal gradients in the ozone field. Both assimilated fields and sondes therefore indicate strong fluctuations of the ozone mixing ratios above Ny-Ålesund and Payerne when filaments pass over the two stations. A few spikes in the assimilated fields of both Odin/SMR and Aura/MLS ozone are however not reproduced in the sonde data. See for example mid-January on the 500 K level at Ny-Ålesund and late January on the 400 K level at Payern. The discrepancies are likely due to imperfections in the modeling of wind driven horizontal transport or the fact that the model is sampled exactly at the station while the sonde may have drifted into another air mass.

4. The 2004/2005 Arctic Polar Vortex

[25] Temperatures observed in the Arctic winter stratosphere of 2004/2005 were the lowest in 50 years, [*European*

Ozone Research Coordinating Unit (EORCU), 2005]. A stable polar vortex was formed by mid-November with temperatures low enough to sustain NAT-type polar strato-spheric clouds, (∼196 K [*Dessler*, 2000]), from early December until the first week of March. The lower boundary of NAT formation temperatures was located around 450 K potential temperature in early December and descended to around 350 K in February. The upper boundary was located around 670 K in mid-December and had descended to around 630 K in late February [*Feng et al.*, 2007].

[26] Planetary wave activity destabilized the polar vortex in the last days of January 2005 causing a minor warming [*EORCU*, 2005]. Vortex average temperatures however remained low until a major rise of vortex temperatures started around 15 February. On 24 February the vortex split, creating two separate vortex centers that reunited around 1 March. During the first week of March, temperatures dropped a few degrees and the vortex remained relatively stable. Thereafter, a second period of rapid warming started. By 11 March the polar vortex started to split for a second time and finally broke up around 22 March.
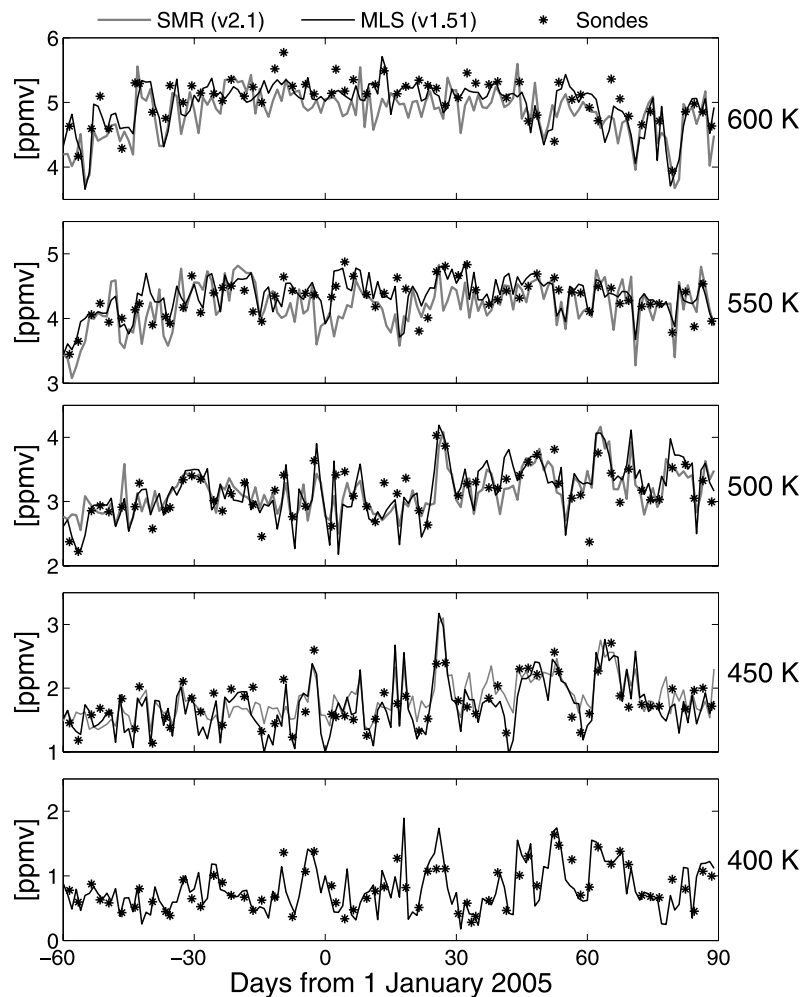
Figure 2. Same as Figure 1 but for comparison at Payerne Switzerland (46°82 N, 6°95 E).

[27] Selected fields of assimilated Aura/MLS ozone are presented in Figure 3. A region with low ozone mixing ratios is clearly visible in the central vortex on the 500 K and 550 K levels during December and January. The region is a remnant of the Arctic summer ozone low [*Fahey and Ravishankara*, 1999] preserved by a central vortex transport barrier at about 75° equivalent latitude that developed in mid-October [*Grooß and Müller*, 2007] before an outer vortex transport barrier was formed at about 65° equivalent latitude. Similar central polar vortex transport barriers have been described in previous Antarctic as well as Arctic early winters, [*Tilmes et al.*, 2006b]. In early February, large scale destabilization of the vortex due to planetary wave activity lead to break down of the central vortex transport barrier. During February the central vortex therefore mixed with the more ozone rich outer vortex. A pronounced central vortex ozone low can thus not be seen in late February and March.

[28] The border of the polar vortex is often defined according to the method described by *Nash et al.* [1996], i.e., by the location of maximum gradient in the potential vorticity field constrained by the location of maximum jet winds. The Nash criterion is for example used in the studies of *Rex et al.* [2006] and *Grooß and Müller* [2007]. According to graphs presented in the study of *Grooß and Müller* [2007], the Nash vortex edge was located within ±2° of 65°

equivalent latitude from early December 2004 up to the vortex break up in mid-March 2005. In this study we therefore use 67° equivalent latitude as vortex border in order to compare vortex areas of equivalent size and at the same time to be sure to remain inside the vortex at all times from 1 January to mid-March. As suggested by *Grooß and Müller* [2007], we furthermore use 75° equivalent latitude to define the central vortex region which is separated from the outer vortex in the early winter. In Figure 4, the inferred vortex borders are compared to assimilated Odin/SMR N_2O fields. The white and black contours in Figure 4 give the 67° and 75° equivalent latitude contours respectively. The white contours coincide well with the maximum gradients in the N_2O tracer fields which indicates that they outline the vortex border. On the 450 K, 500 K and 550 K levels, the black contours outline central vortex regions with low N_2O mixing ratios compared to the outer vortex in December and January. Since the inner vortex barrier subsequently broke down, the black contours do not outline any specific regions of the vortex in February and March.

[29] Figure S1 in the auxiliary material[1] for this article corresponds to Figure 4 but has been made by assimilating

---

[1]Auxiliary materials are available in the HTML. doi:10.1029/2007JD009560.
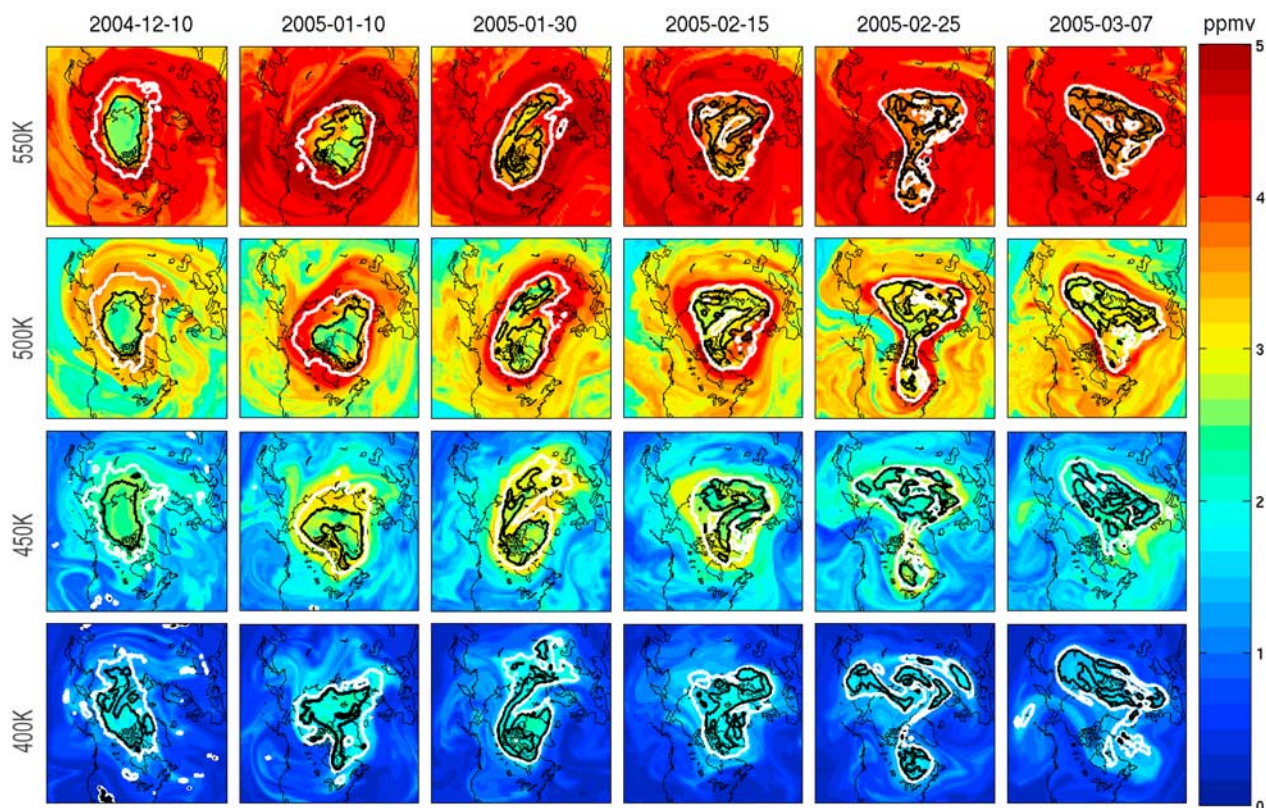
Figure 3. Fields of assimilated Aura/MLS ozone from the Arctic winter of 2004/2005. The four rows describe the ozone mixing ratios on the 400 K, 450 K, 500 K, and 550 K potential temperature levels on the dates given on top of each column. The white and black contours in each panel define the 67° and 75° equivalent latitude contours, respectively.

N_2O data from Aura/MLS. Figures 4 and S1 show qualitatively the same horizontal distribution of N_2O and the white contours coincide with the maximum gradients in the tracer fields which indicates that the lines outline the vortex border.

[30] Because of radiative cooling, potential temperatures of air masses in the polar region fall during autumn and winter. When estimating polar ozone depletion on isentropic levels (i.e., potential temperature levels), it is essential to compensate for this cross-isentropic transport since ozone mixing ratios in the lower stratosphere generally rise with altitude up to an ozone maximum, normally located above 800 K potential temperature.

[31] One method of estimating cross-isentropic transport in the polar vortex is to monitor the descent of chemically inert tracer species. In this study, nitrous oxide (N_2O) from Aura/MLS and Odin/SMR have been used to estimate the vertical transport. The mixing ratio of N_2O decreases rapidly with altitude since it is destroyed by $O(1_D)$ and dissociated by high-energy UV radiation in sunlit regions of the upper stratosphere. The constituent is on the other hand chemically inert at lower altitudes and in the polar night and can therefore be used as a passive tracer to monitor transport in the polar vortex.

[32] Daily vortex averages of Aura/MLS and Odin/SMR N_2O measurements are plotted in Figure 5. The dashed lines are 5-day running averages of the N_2O mixing ratios north of 75° equivalent latitude and the solid lines are 5-day running averages of the mixing ratios in the outer regions of the vortex between 67° and 75° equivalent latitudes. Aura/MLS data are plotted in Figure 5 (top) and Odin/SMR data are plotted in Figure 5 (bottom). The sinking N_2O mixing ratios in November, December and January indicate cross-isentropic transport due to radiative cooling in the polar vortex. The dashed lines furthermore show that N_2O mixing ratios were lower in the central vortex than in the outer vortex from the formation of the vortex in mid-November to late February. By 15 February the N_2O mixing ratios in the central vortex started to rise, finally reaching the mixing ratios found in the outer vortex by early March which is consistent with the inner vortex transport barrier breaking down in early February, as indicated by the black contours in Figure 4, allowing mixing within the vortex to occur. The rising N_2O mixing ratios in the central vortex could possibly also have been explained by vertical transport but the agreement between N_2O mixing ratios in the inner and outer vortex suggests that intravortex mixing is the likely cause of the phenomenon.

5. Model Estimates of Cross-Isentropic Transport

[33] To analyze cross-isentropic transport we use the DIAMOND transport model. By comparing assimilated fields of N_2O to passively transported fields we can determine if the cross-isentropic transport rates used in the passive transport model are correct. The passive fields are
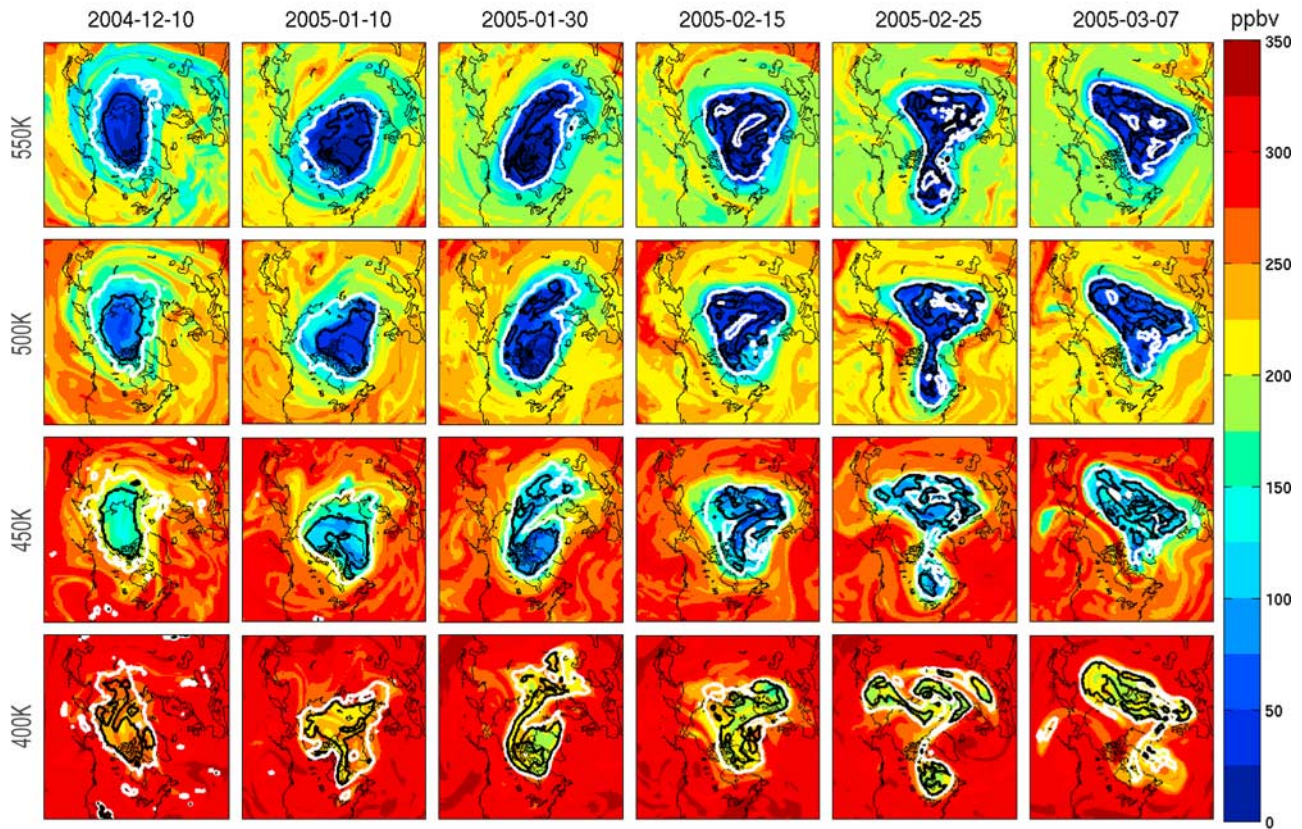
Figure 4. Fields of assimilated Odin/SMR N_2O from the Arctic winter of 2004/2005. The four rows describe the N_2O mixing ratios on the 400 K, 450 K, 500 K, and 550 K potential temperature levels on the dates given on top of each column. The white and black contours in each panel define the 67° and 75° equivalent latitude contours, respectively.
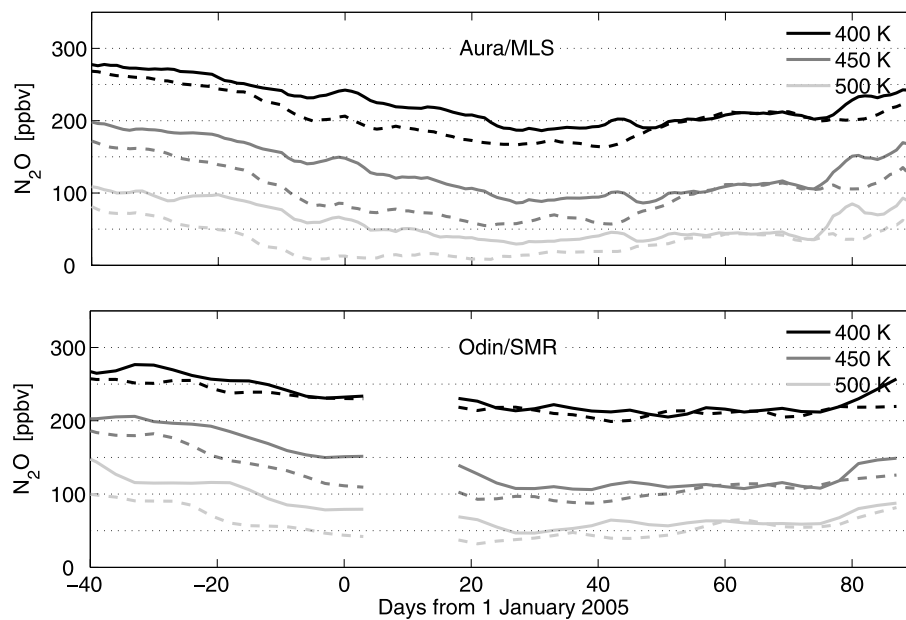

Figure 5. Average N_2O mixing ratios on three different potential temperature levels in the Arctic polar vortex of 2004/2005. (top) Aura/MLS data and (bottom) Odin/SMR data. The dashed lines represent the average mixing ratios in the central vortex located north of 75° equivalent latitude, and the solid lines represent the average mixing ratios in the outer vortex between 67° and 75°. Odin/SMR data are not available for a period in early January.

Table 1. Summary of Vortex Average Descent Rates Estimated by Assimilating N_2O From Odin/SMR and Aura/MLS in the DIAMOND Model[a]

Potential Temperature	1 Jan to 14 Feb		15 Feb to 31 Mar	
	Odin/SMR N_2O	Aura/MLS N_2O	Odin/SMR N_2O	Aura/MLS N_2O
400 K	0.6	0.6	0.1	−0.2
450 K	0.7	0.7	0.1	−0.3
500 K	1.1	1.1	0.2	0.0
550 K	1.5	1.6	0.3	0.3
600 K	2.0	2.1	0.6	0.5
650 K	2.4	2.5	1.1	1.1
700 K	3.0	3.0	1.7	1.7

[a]The rates are given in potential temperature K/d.

initialized by assimilating N_2O from August to 31 December 2004. Subsequently we use two different methods for implementing vertical transport in the DIAMOND model.

[34] First we let the entire vortex region north of 50° equivalent latitude descend at a rate that is independent of location. The rate of descent is chosen so the vortex average N_2O mixing ratios in the passive transport model agree with assimilated fields. For January and the first 2 weeks of February, best agreement between passive and assimilated N_2O mixing ratios are obtained when implementing vertical transport at a rate of 0.6–0.8 K/d below 500 K, with 1.1–2.1 K/d between 500 K and 600 K and with 2.1–3.0 K/d above 600 K. Assimilating Odin/SMR or Aura/MLS N_2O data makes no significant difference to the analysis during this period. Both sets of data furthermore indicate that the rates of cross-isentropic transport decrease after 14 February. Different descent rates are however obtained depending on whether data from Odin/SMR or Aura/MLS are assimilated after 14 February. Best agreement between passive and assimilated Odin/SMR N_2O mixing ratios are obtained by letting the vortex descend at a rate of 0.1–0.2 K/d below 500 K, by 0.2–0.6 K/d between 500 K and 600 K and by 0.6–1.7 K/d above 600 K. Best agreement between passive and assimilated Aura/MLS N_2O mixing ratios are on the other hand obtained by allowing potential temperatures to increase by 0.2–0.3 K/d below 500 K, by letting potential temperatures decrease by 0–0.5 K/d between 500 K and 600 K and by letting potential temperatures decrease by 0.6–1.7 K/d above 600 K. The estimated descent rates are summarized in Table 1.

[35] Secondly, we implement cross-isentropic transport using diabatic cooling rates derived from the SLIMCAT CTM model [*Feng et al.*, 2007] which used the NCAR CCM radiation scheme [*Feng et al.*, 2005; *Briegleb*, 1992]. The NCAR CCM radiative scheme is used by both *Rex et al.* [2006] and *Singleton et al.* [2007] in their studies of 2004/2005 Arctic ozone depletion. We have therefore included it in this study to facilitate comparison with their results as well as for validating the vortex descent method described above. Diabatic cooling rates were derived once per day for every grid point in the SLIMCAT model. The SLIMCAT diabatic cooling rates were then linearly interpolated to the grid in the DIAMOND model and used to implement full 3-D transport. Temperature fields from ECMWF were used in the SLIMCAT model when calculating the diabatic cooling rates. The diabatic cooling rates are equivalent to the rates in the study by *Singleton et al.* [2007].

[36] Assimilated fields of Odin/SMR and Aura/MLS N_2O are compared to passively transported N_2O fields in Figures 6 and 7. The solid lines represent assimilated N_2O north of 67° equivalent latitude while the dashed and dash-dotted lines represent vortex average N_2O mixing ratios in passive fields where cross-isentropic transport is implemented using vortex descent and diabatic cooling rates from SLIMCAT
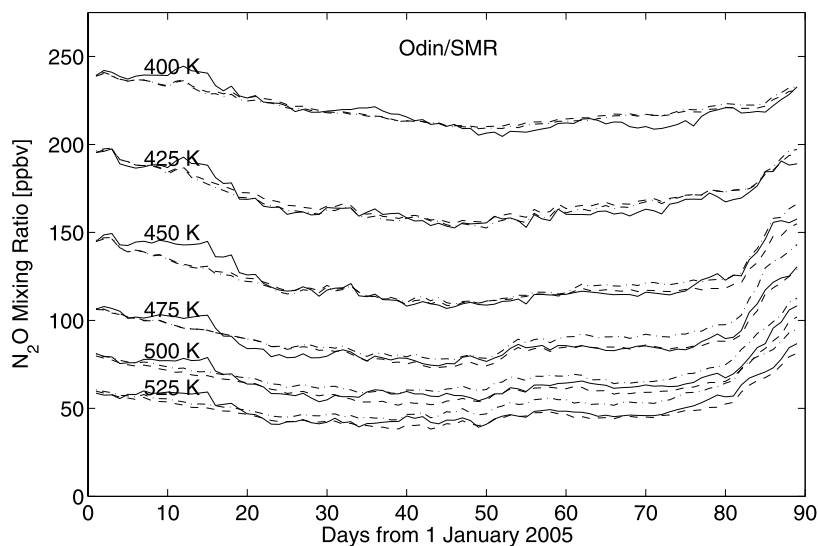

Figure 6. Vortex average N_2O mixing ratios in the DIAMOND model. The solid lines display vortex averages of assimilated Odin/SMR N_2O data while the dashed and dash-dotted lines display vortex averages from fields passively transported from 1 January 2005. The dashed lines represent passive fields where cross-isentropic transport was implemented using the vortex descent method while the dash-dotted lines come from fields where cross-isentropic transport was implemented using diabatic cooling rates from a radiative scheme.
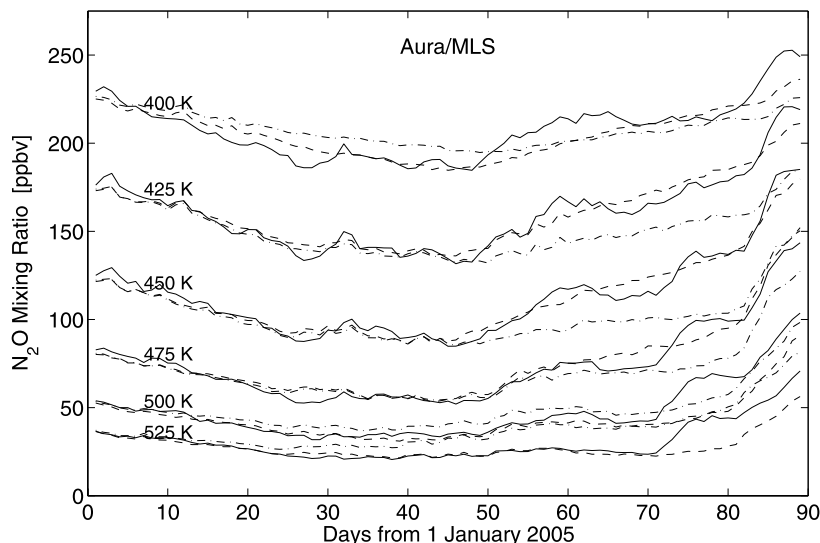
Figure 7. Vortex average N$_2$O mixing ratios in the DIAMOND model. The solid lines display vortex averages of assimilated Aura/MLS N$_2$O data while the dashed and dash-dotted lines display vortex averages from fields passively transported from 1 January 2005. The dashed lines represent passive fields where cross-isentropic transport was implemented using the vortex descent method while the dash-dotted lines come from fields where cross-isentropic transport was implemented using diabatic cooling rates from a radiative scheme.

respectively. The vertical transport rates used for the dashed lines were chosen to fit the respective solid lines. Odin/SMR data are not available between days 5 and 15 so there are some discrepancies between dashed and solid lines in the Odin/SMR plot during this period. Good agreement between dashed and solid Odin/SMR lines are however seen subsequently. The dash-dotted lines also agree well to the solid Odin/SMR lines indicating that both tuned vortex descent and the SLIMCAT diabatic heating rates give similar cross-isentropic transport. The dashed and dash-dotted Aura/MLS lines also show good agreement with the assimilated fields in January and early February. Below

500 K, the dash-dotted lines however indicate lower N$_2$O mixing ratios than the assimilated solid lines after day 45.

[37] The vortex average mixing ratios of assimilated Aura/MLS and Odin/SMR N$_2$O are compared in Figure 8. In January and the two first weeks of February the Aura/MLS N$_2$O mixing ratios are ~20 ppbv lower than the Odin/SMR mixing ratios on the potential temperature levels displayed. On the 400 K, 425 K and 450 K potential temperature levels the Aura/MLS N$_2$O mixing ratios however rise after mid-February reaching levels that agree with the Odin/SMR N$_2$O mixing ratios by the end of February. The Aura/MLS N$_2$O mixing ratios also rise on the 475 K and 500 K levels but do not reach the levels in the Odin/
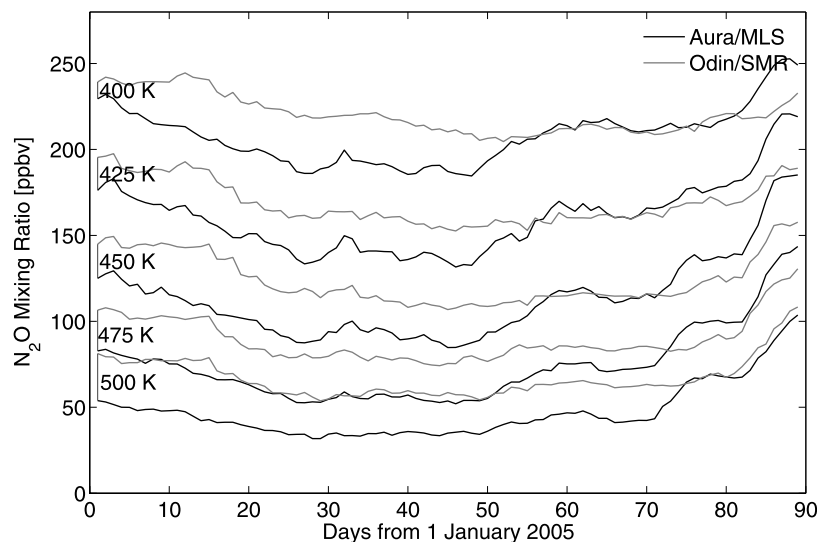

Figure 8. Comparison of Aura/MLS to Odin/SMR N$_2$O mixing ratios in the polar vortex. The graphs describe the average N$_2$O mixing ratios north of 67° equivalent latitude in the DIAMOND model.
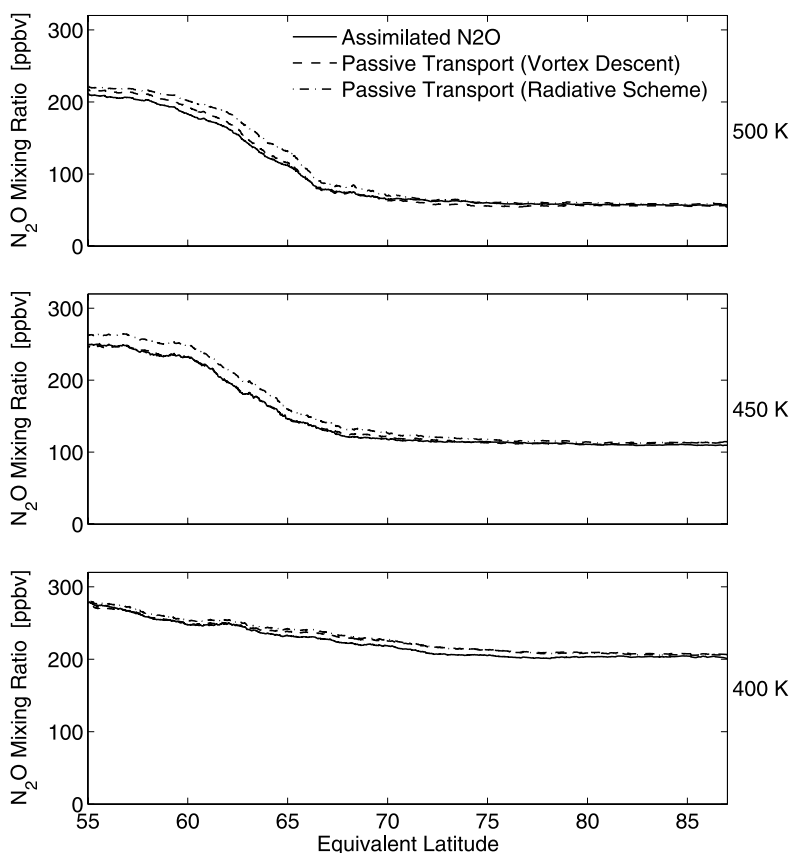
Figure 9. The three graphs describe the Odin/SMR N_2O mixing ratios in the DIAMOND model on 14 March 2005 as functions of equivalent latitude on the 500 K, 450 K, and 400 K potential temperature levels. The solid lines come from assimilated N_2O fields while the dashed and dash-dotted lines come from N_2O in fields passively transported from 1 January 2005. The dashed lines come from passive fields where cross-isentropic transport is implemented using the vortex descent method while the dash-dotted lines come from fields where cross-isentropic transport is implemented using diabatic cooling rates from a radiative scheme.

SMR fields until the vortex breaks up in mid-March. Both Aura/MLS and Odin/SMR N_2O mixing ratios furthermore rise in the latter half of March as the polar vortex breaks up and N_2O rich extra vortex air enters it.

[38] The rising Aura/MLS N_2O mixing ratios are interpreted as ascent of the vortex in the vortex "descent" study above. The Odin/SMR N_2O mixing ratios do on the other hand not rise in late February so the Odin/SMR vortex descent study does not indicate any vortex ascent in that period. Furthermore, the cross-isentropic transport rates from the SLIMCAT model corroborate the Odin/SMR descent rates and do not indicate vortex ascent in late February. Since the vertical gradients of Aura/MLS N_2O mixing ratios inside the vortex drop more rapidly as a function of altitude after mid-February than in the early winter, the rising N_2O mixing ratios in the lower vortex could possibly be explained by increased exchange of air masses across the vortex border at low altitudes. For this explanation to be true, the cross vortex border exchange would however have had to be stronger than seen in the passive DIAMOND model and it is furthermore not corroborated by the Odin/SMR N_2O measurements. As mentioned in section 2.2 of this manuscript, significant discrepancies exist between the version 1.5 Aura/MLS N_2O data used in this study and the more recently

produced version 2.2 of the data. Therefore we suggest that the rapid rise of N_2O mixing ratios in late February and early March is possibly an artefact in the version 1.5 Aura/MLS N_2O data.

[39] Figures 9 and 10 describe the Odin/SMR and Aura/MLS N_2O mixing ratios in the DIAMOND model on 14 March 2005 as functions of equivalent latitude on the 500 K, 450 K, and 400 K potential temperature levels. Assimilated N_2O fields are compared to N_2O fields passively transported from 1 January 2005. The assimilated fields are compared to passive fields with cross-isentropic transport implemented using the vortex descent method and to fields with cross-isentropic transport implemented using diabatic cooling rates taken from SLIMCAT.

[40] The vortex descent fields (dashed lines) agree well to the assimilated Odin/SMR and Aura/MLS N_2O fields at all equivalent latitudes in Figures 9 and 10. The tuning of vortex descent rates is thus not very sensitive to the equivalent latitude used to define the edge of the polar vortex.

[41] In Figure 9, the dash-dotted lines representing the case of cross-isentropic transport implemented using diabatic cooling rates taken from SLIMCAT agree with the solid Odin/SMR lines north of 67° equivalent latitude while
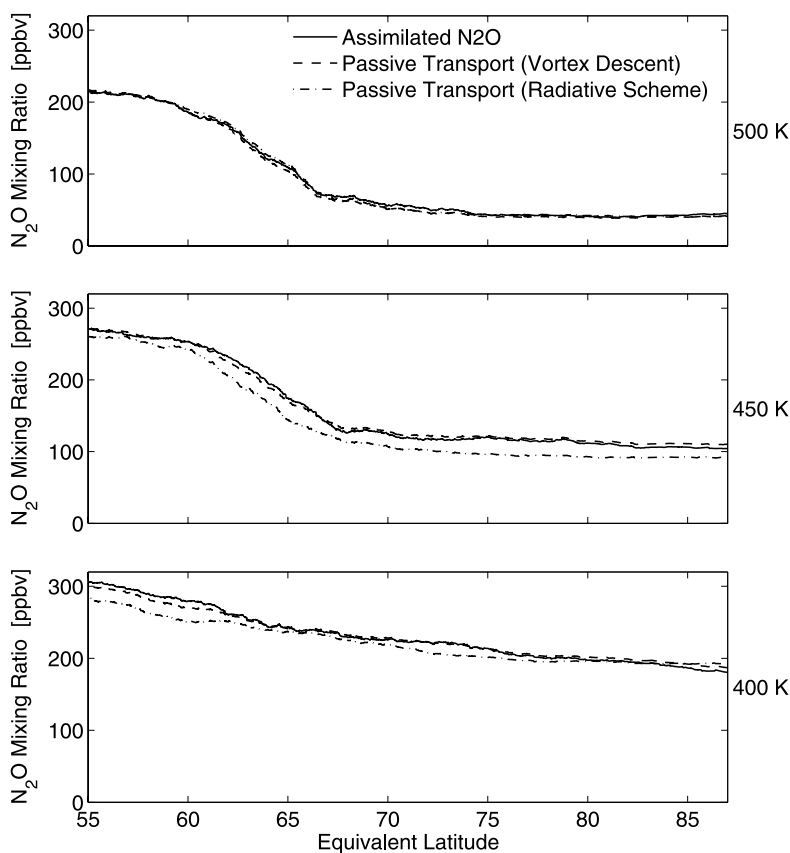
Figure 10. Like Figure 9 but with Aura/MLS N_2O.

they are a bit higher than the solid lines south of 67° equivalent latitude on the 450 K and 500 K levels. In Figure 10, the dash-dotted lines on the other hand agree with the solid assimilated Aura/MLS N_2O fields on the 500 K level while they are below the solid lines at all equivalent latitudes on the 450 K level. On the 400 K level the dash-dotted lines agree with the solid lines in most regions of the inner vortex while they are below the assimilated Aura/MLS N_2O fields south of 62° equivalent latitude. Significant differences thus exist between the Odin/SMR and Aura/MLS N_2O tracers and the SLIMCAT diabatic cooling rates although the SLIMCAT rates agree with Odin/SMR N_2O north of 67° equivalent latitude.

6. Vortex Average Ozone Decline

[42] The time evolution of the ozone mixing ratios in the central and outer vortex regions are plotted in Figure 11. The dashed lines are 5-day running averages of all satellite ozone measurements in the central vortex located north of 75° equivalent latitude and the solid lines are 5-day running averages of the ozone measurements in the outer vortex between 67° and 75° equivalent latitude. Aura/MLS data are plotted in Figure 11 (top) and Odin/SMR data are plotted in Figure 11 (bottom). To compensate for cross-isentropic transport, the satellite ozone profiles have been interpolated on to N_2O isopleths using the N_2O profiles that are retrieved in parallel with each ozone profile.

[43] From the end of December to early March, the Aura/MLS graphs in Figure 11 indicate falling ozone mixing ratios in the outer vortex. The largest decline can be seen on the 100 ppbv isopleth where the graphs indicate that ozone mixing ratios fell by ~1.5 ppmv which is of the same order as the ~2.0 ppmv ozone loss in the outer vortex estimated by *Manney et al.* [2006]. Falling ozone mixing ratios can also be seen in the inner vortex although the decline is smaller. The maximum decline in the inner vortex can be seen on the 150 ppbv isopleth where ozone mixing ratios fell by ~0.8 ppmv. The Odin/SMR graphs are more noisy but declining ozone mixing ratios can be seen in the outer as well as the inner polar vortex. The maximum decline in ozone mixing ratios can be found on the 100 ppbv and 150 ppbv isopleths just as in the Aura/MLS graphs and amounts to ~0.9 ppmv and ~0.8 ppmv in the outer and inner vortex respectively. It should however be noted that large disagreement in vortex N_2O mixing ratios is found between the Aura/MLS and Odin/SMR instruments (see section 5). Figure 11 should therefore not be seen as a comparison of the ozone mixing ratios retrieved using the two different instruments but rather as an indicator of what ozone depletion estimates can be expected in the outer and central vortex regions in studies based on correlation of ozone to the inert N_2O tracer.

[44] Catalytic ozone depletion taking place when sunlight returned to the polar region in the late winter caused most of the perceived large scale decline of the outer vortex ozone mixing ratios. A substantial part of the decline of ozone in
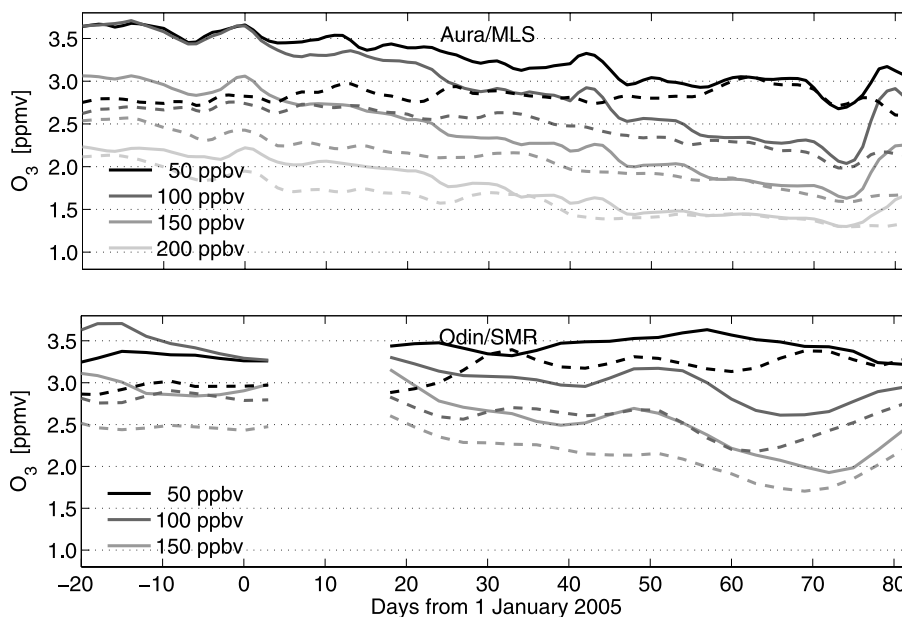
Figure 11. Average ozone mixing ratios on different N_2O isopleths in the Arctic polar vortex of 2004/2005. (top) Data from Aura/MLS and (bottom) data from Odin/SMR. The dashed lines represent the average mixing ratios in the central vortex located north of 75° equivalent latitude, and the solid lines represent the average mixing ratios in the outer vortex between 67° and 75° equivalent latitude. The measurement response of Odin/SMR 501.5 GHz ozone data is generally below 0.7 on the 200 ppbv N_2O isopleth. It has therefore not been included in the graph.

the outer vortex that is indicated in Figure 11 can however be attributed to the outer vortex mixing with ozone poor air from the central vortex, see Figure 3. Intravortex mixing furthermore introduced N_2O poor central vortex air into the outer vortex causing overcompensation for vertical transport. Any decline of ozone mixing ratios due to photochemical ozone depletion in the central vortex must have likewise been underestimated because of intravortex mixing. Intrusions of extra vortex air masses into the vortex may furthermore have influenced the ozone loss estimates in the vortex. Extra vortex air however leads to overestimation of ozone losses since N_2O mixing ratios in extra vortex air are higher than inside the vortex although ozone mixing ratios are lower.

[45] Since photochemical ozone depletion and intravortex mixing both occur in concert with rising insolation rates in the late polar winter it is difficult to separate the two effects inside the vortex. Estimating the average ozone loss for the entire vortex is on the other hand reasonable as long as one samples both inner and outer vortex regions. The time evolution of the ozone mixing ratios in the entire vortex north of 67° equivalent latitude is presented in Figure 12. Aura/MLS data are plotted in Figure 12 (top) and Odin/SMR data are plotted in Figure 12 (bottom). The potential temperatures corresponding to the N_2O isopleths are given in Figure 13.

[46] By day 73 of the year 2005, the Aura/MLS graphs indicate ~0.4 ppmv, ~1.1 ppmv, ~1.0 ppmv and ~0.8 ppmv ozone loss compared to late 2004 on the 50 ppbv, 100 ppbv, 150 ppbv and 200 ppbv N_2O isopleths. After day 73 the graphs indicate additional ozone loss, but the decline coincides with break up of the vortex that causes extra vortex air with different O_3/N_2O ratios to enter the

remnants of the vortex and thus interfere with the tracer correlation analysis. The Odin/SMR graphs indicate ~0.2 ppmv rise of the ozone mixing ratios on the 50 ppbv isopleth and ~0.7 ppmv and ~0.9 ppmv ozone loss on the 100 ppbv and 150 ppbv N_2O isopleths by day 73 of 2005 compared to late 2004.

[47] The large scale decline of ozone mixing ratios seen in Figure 12 can only be explained by photochemical ozone depletion. To fully account for all causes behind the decline it is however also necessary to include intrusions of extravortex air across the 67° equivalent latitude contour in the analysis. On potential temperature levels below ~500 K, extravortex air has substantially lower ozone mixing ratios than air masses in the outer vortex (see Figure 3). Intrusion of extravortex air in January, February and early March of 2005 can therefore have contributed to the decline of ozone mixing ratios in the vortex. Intrusion of extravortex air however also leads to increasing N_2O mixing ratios which in turn leads to undercompensation for cross-isentropic descent and consequently to underestimation of photochemical ozone loss since ozone mixing ratios increase with altitude in the lower stratosphere [*Müller et al.*, 2005].

7. Model Estimates of Ozone Depletion

[48] The photolytic destruction of ozone occurring in January, February and March is estimated by comparing assimilated fields of ozone to model fields transported from 1 January onward without having satellite data assimilated into them north of the 30° N parallel. The initial fields on 1 January are obtained by running the DIAMOND model with full assimilation of satellite data from 13 August of 2004 to that date. In this study, vertical transport is imple-
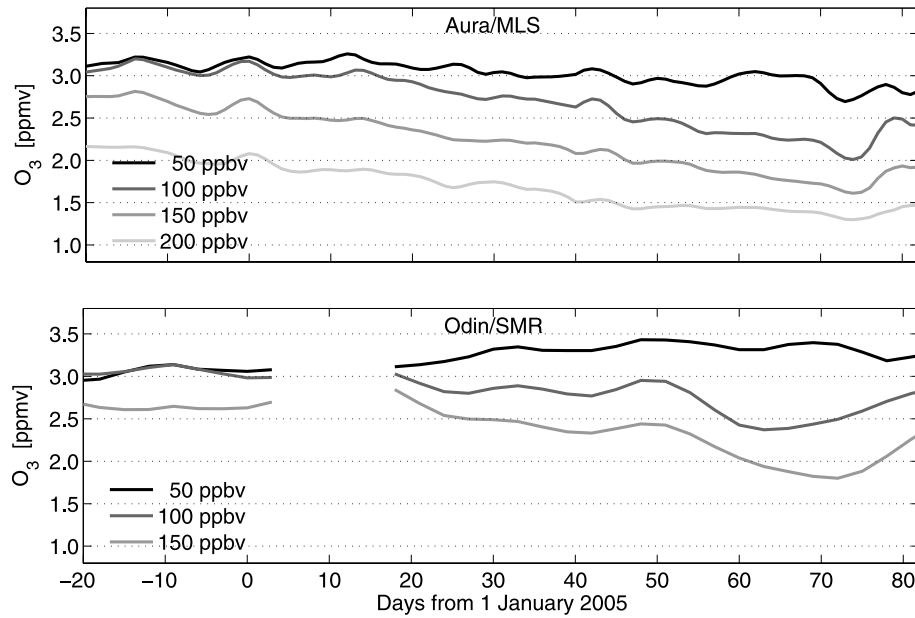
Figure 12. Average ozone mixing ratios on different N_2O isopleths in the Arctic polar vortex of 2004/2005. (top) Data from Aura/MLS and (bottom) data from Odin/SMR. The lines represent the average mixing ratios in the polar vortex defined as the area north of 67° equivalent latitude. Odin/SMR ozone data are not available on the 200 ppbv N_2O isopleth.

mented using both diabatic cooling rates from the SLIM-CAT model as well as the vortex descent method described in section 5. Since temperatures low enough to sustain polar stratospheric clouds were not recorded above 650 K past 1 January 2005, [*Feng et al.*, 2007], we assume that heterogenous polar processing of chlorine reservoir species did not cause ozone depletion above that level. Satellite ozone data has therefore been assimilated on and above the 675 K level in the passive transport fields. It is possible that ozone was

lost above 650 K in chemical reactions not involving anthropogenic chlorine. Assimilating ozone data above the upper range of polar stratospheric clouds is a way of separating out such processes from this study so attention can be focused on chlorine catalyzed ozone depletion at lower altitudes. In the DIAMOND model, satellite data is assimilated separately on each vertical level with no correlations between different potential temperature levels. The assimilation of ozone data on and above the 675 K level is
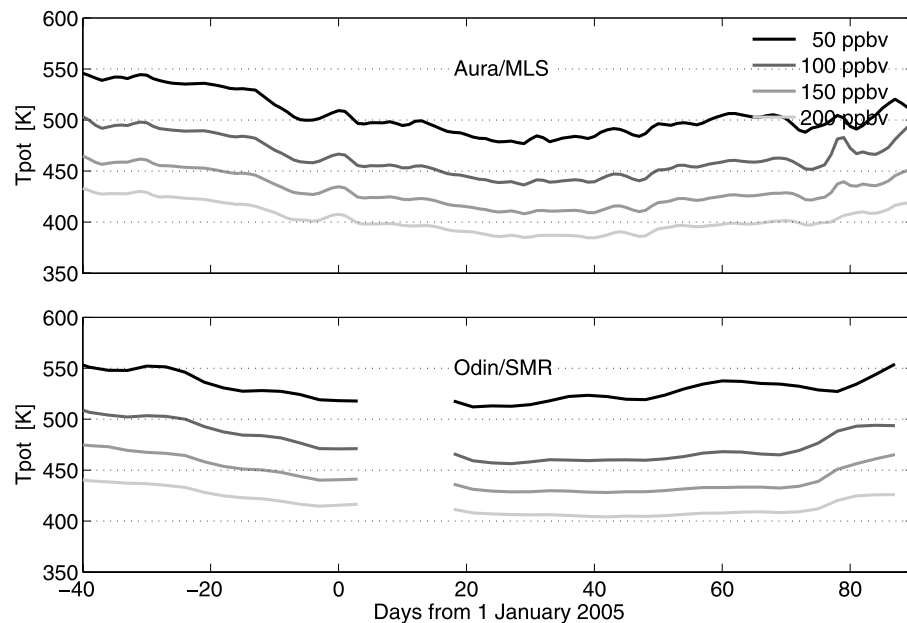

Figure 13. Average potential temperatures north of 67° equivalent latitude on different N_2O isopleths in the Arctic polar vortex of 2004/2005. (top) Isopleths from Aura/MLS data and (bottom) isopleths from Odin/SMR data. Odin/SMR data are not available for a period in early January.
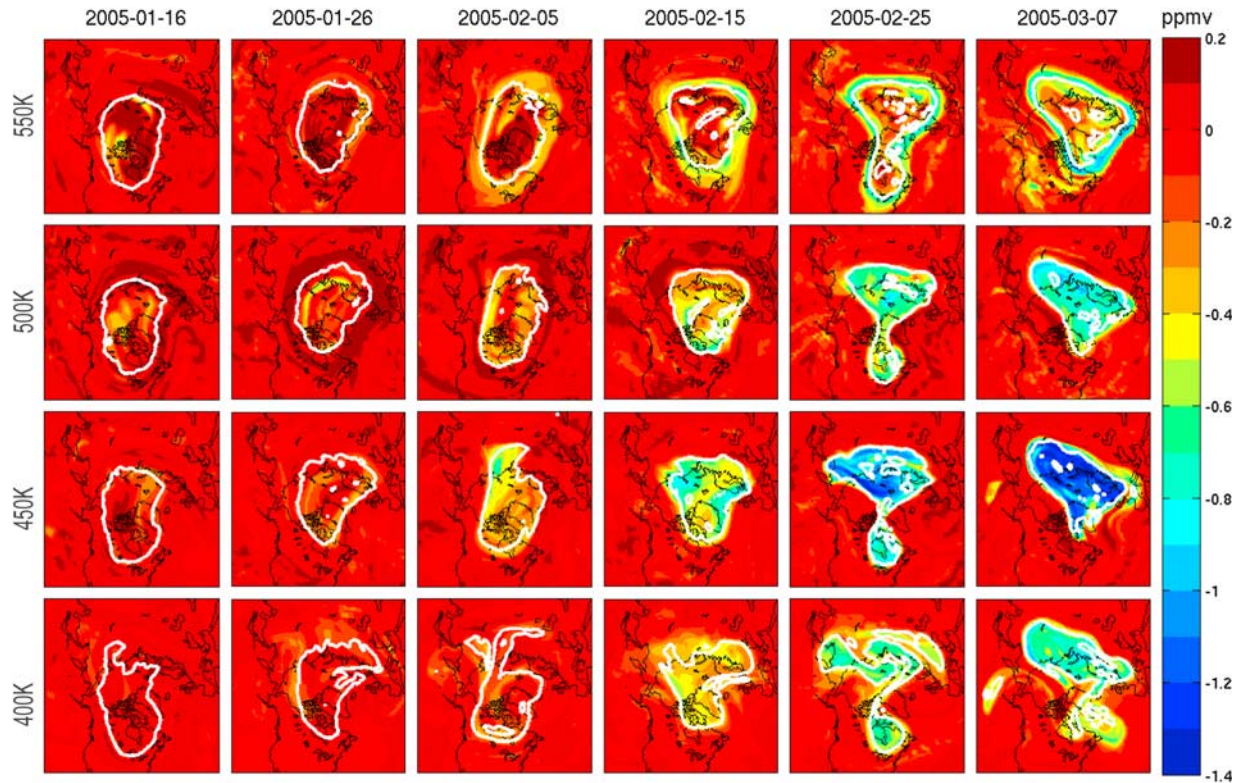
Figure 14. Estimates of ozone depletion in the Arctic spring of 2005 made by subtracting model fields passively transported from 1 January from assimilated fields of Aura/MLS data. The solid white lines give the 67° equivalent latitude.

therefore not influenced by the passively transported levels below. On the 675 K level in the DIAMOND model, the assimilated Aura/MLS vortex average ozone mixing ratios are typically 0.0–0.1 ppmv higher than the assimilated Odin/SMR vortex average ozone mixing ratios. Any discrepancies between ozone loss estimates based on assimilation of Aura/MLS and Odin/SMR data can therefore not be explained by differing ozone mixing ratios being assimilated on the higher potential temperature levels of the model.

[49] The ozone losses found using Aura/MLS and Odin/SMR data are mapped and quantified in Figures 14 and 15. Figures 14 and 15 have been obtained by subtracting the DIAMOND fields that were modeled without assimilation north of the 30° N parallel from model fields that were continuously updated by assimilation of incoming satellite data in the polar region. Vertical transport was implemented using diabatic cooling rates from the SLIMCAT model. The solid white lines give the 67° equivalent latitude.

[50] The 400 K level was only studied using Aura/MLS data since Odin/SMR ozone data have too low measurement response at this level. By 26 January, traces of ozone loss can be seen around the vortex edge on the 400 K level but large scale depletion did not start until February. By 7 March, ozone losses in the range 0.5–0.9 ppmv can be seen in the vortex dependent on location.

[51] On the 450 K level, small areas with ozone depleted vortex air can be seen by 26 January in the Odin/SMR fields while little ozone destruction can be observed in the Aura/MLS fields. Both instruments indicate that large scale ozone destruction occurred in the entire vortex throughout February. On 25 February and 7 March the Aura/SMR fields indicate more severe ozone depletion than the Odin/SMR fields. By 7 March, the Aura/MLS fields indicate ozone depletion in the range 1.0–1.4 ppmv while Odin/SMR fields show ozone depletion in the range 0.8–1.2 ppmv in the central vortex with less depletion around the outer edges of the vortex. Keeping in mind that the altitude resolution of the Odin/SMR ozone profiles is ~3 km, it is possible that the difference is due to the 450 K potential temperature level being close to low altitudes where the Odin/SMR 501.5 GHz ozone profiles have low measurement response.

[52] The ozone depletion on the 500 K level was similar to that on the 450 K level. The Aura/MLS fields indicate little ozone depletion before 5 February while the Odin/SMR fields indicate small regions of ozone depleted air in the central vortex on 26 January. By 15 February the Aura/MLS field indicate ozone depletion evenly distributed over the vortex while the Odin/SMR fields indicate strong depletion in some areas while no depletion at all can be seen in other vortex regions. By 25 February, ozone depleted air is seen in the entire vortex. By 7 March, the Aura/MLS field indicate ozone losses in the range 0.6–0.9 ppmv while the Odin/SMR fields indicate losses in the range 0.4–1.0 ppmv dependent on location in the vortex.
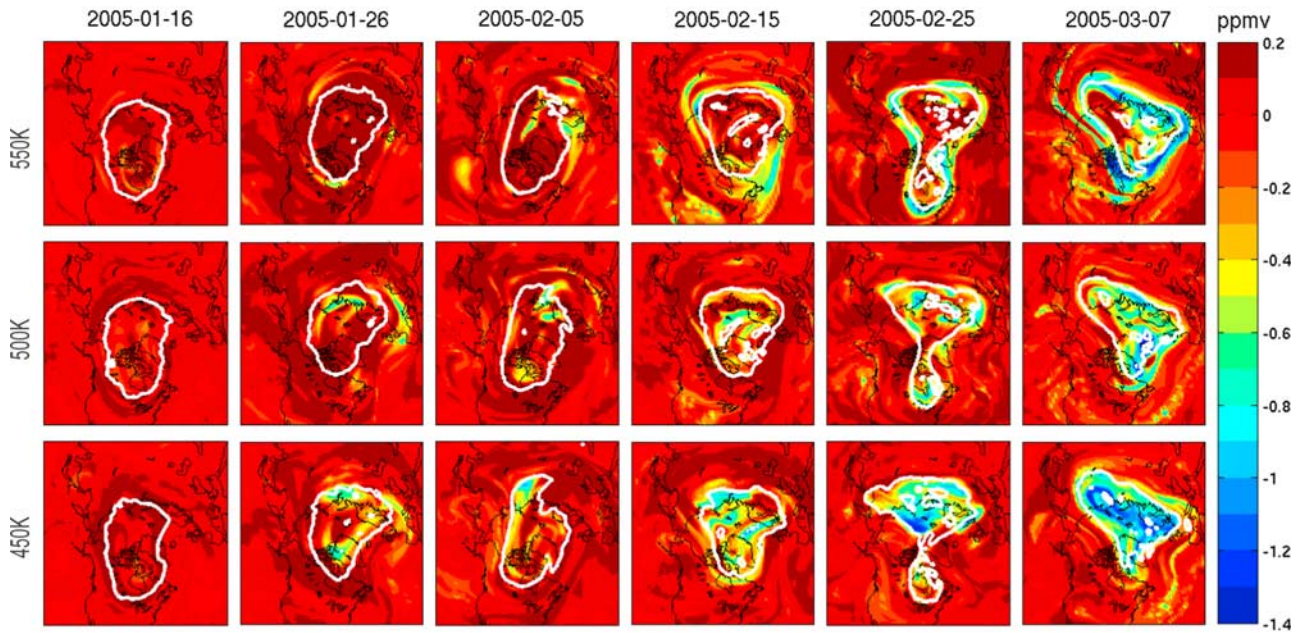
Figure 15. Estimates of ozone depletion in the Arctic spring of 2005 made by subtracting model fields passively transported from 1 January from assimilated fields of Odin/SMR data. The solid white lines give the 67° equivalent latitude.

[53] Both Aura/MLS and Odin/SMR fields indicate that ozone depletion was strongest in regions near the vortex border on the 550 K level. The Aura/MLS fields indicate a distinct band with 0.2–0.3 ppmv ozone losses around the vortex by 5 February while 0.4–0.6 ppmv ozone depletion can be seen in small regions near the vortex edge in the Odin/SMR fields. By 7 March the Aura/MLS field indicates ozone depletion in the range 0.5–1.0 ppmv around the vortex border while the Odin/SMR field indicates ozone depletion in the range 0.8–1.2 ppmv in the same region.

[54] Daily vortex averages of the difference between assimilated and passively transported ozone fields are presented in Figure 16. Results from assimilated Aura/MLS data are plotted in Figure 16 (top) and results from assimilated Odin/SMR data in Figure 16 (bottom). The solid lines are obtained by implementing cross-isentropic trans-
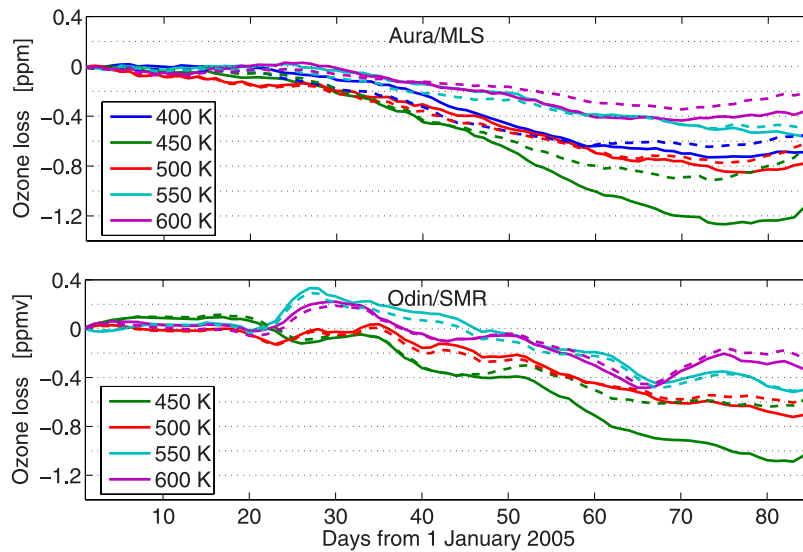

Figure 16. Average losses of ozone mixing ratios north of 67° equivalent latitude in the DIAMOND model. (top) Results from assimilated Aura/MLS data and (bottom) results from assimilated Odin/SMR data. The solid lines are obtained when implementing cross-isentropic transport using diabatic cooling rates from the SLIMCAT model, and the dashed lines are obtained when implementing cross-isentropic transport using a vortex descent method based on vertical transport rates inferred from Aura/MLS N_2O data.
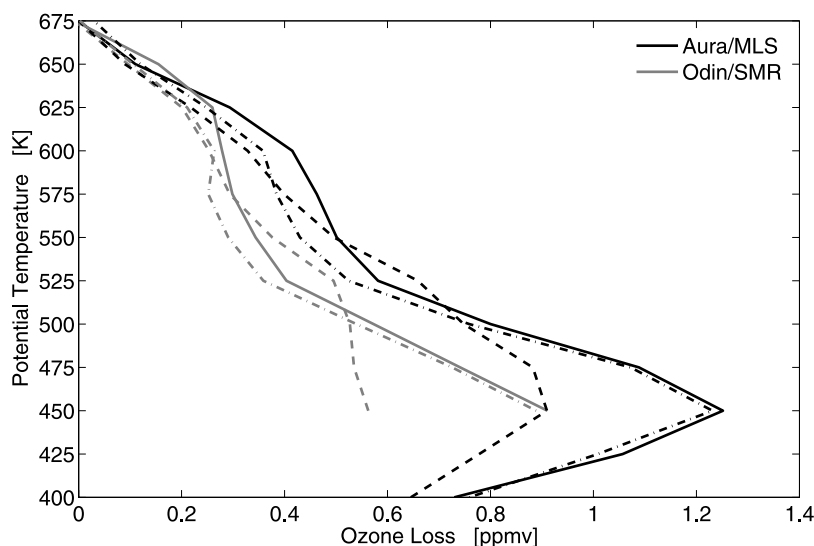
Figure 17. Model estimates of vortex average ozone losses north of 67° equivalent latitude on 14 March 2005. The solid lines are obtained when vertical transport is implemented using diabatic cooling rates from the SLIMCAT model. The dashed lines are obtained by implementing cross-isentropic transport using a vortex descent method based on vertical transport rates inferred by Aura/MLS N_2O data while the dash-dotted lines are obtained on the basis of vertical transport rates inferred by Odin/SMR N_2O data.

port using diabatic cooling rates from the NCAR CCM radiative scheme in the SLIMCAT model and the dashed lines are obtained when implementing cross-isentropic transport using the vortex descent method with descent rates derived from Aura/MLS N_2O data. Results from implementing cross-isentropic transport using the vortex descent method with descent rates derived from Odin/SMR N_2O data are very similar to the NCAR CCM radiative scheme results and have therefore not been included. The graphs are smoothed using a 5-day running average.

[55] The Aura/MLS panel indicates that ozone depletion started ~20 January on most levels although some loss of ozone can be observed before that date on the 500 K level. Large scale ozone destruction can subsequently be seen during February and early March until day 75 when the vortex starts to break up. On the 450 K level there are significant differences between the ozone depletion estimates obtained using vortex descent based on Aura/MLS N_2O data and diabatic cooling rates from SLIMCAT model. The discrepancy becomes visible after mid-February when cross-isentropic ascent is inferred in the Aura/MLS N_2O study in section 5. By 14 March 2005, (day 73), the solid "diabatic cooling" graphs indicate 0.7 ppmv, 1.3 ppmv, 0.8 ppmv, 0.5 ppmv and 0.4 ppmv average depletion on the 400 K, 450 K, 500 K, 550 K and 600 K levels while the dashed "vortex descent" graphs indicate 0.6 ppmv, 0.9 ppmv, 0.7 ppmv, 0.5 ppmv and 0.3 ppmv average depletion on the 400 K, 450 K, 500 K, 550 K and 600 K levels.

[56] The Odin/SMR graphs in Figure 16 (bottom) are more noisy but ozone destruction can be seen in February and March. By 14 March 2005, the Odin/SMR "diabatic cooling" graphs indicate 0.9 ppmv, 0.6 ppmv, 0.4 ppmv and 0.3 ppmv average depletion on the 450 K, 500 K, 550 K and 600 K levels while the dashed "vortex descent" graphs

indicate 0.6 ppmv, 0.5 ppmv, 0.4 and 0.3 ppmv vortex average ozone depletion on the 450 K, 500 K, 550 K and 600 K levels.

[57] Vertical profiles of vortex average ozone loss north of 67° equivalent latitude between 1 January and 14 March 2005 are presented in Figure 17. Ozone losses estimated using Odin/SMR data are generally lower than estimates based on Aura/MLS data. The discrepancy is likely a consequence of Odin/SMR 501.5 GHz ozone data having low measurement response in the lowermost stratosphere. Typically, Odin/SMR 501.5 GHz ozone have measurement response of ~70% on the 450 K level, of ~75% on the 475 K level and of ~85% on the 500 K level. On most potential temperature levels we furthermore estimate stronger ozone loss when cross-isentropic transport is implemented by vortex descent tuned to assimilated Odin/SMR N_2O than we estimate when cross-isentropic transport is implemented by vortex descent tuned to assimilated Aura/MLS N_2O. Below 525 K the ozone losses derived when cross-isentropic transport is implemented by vortex descent tuned to assimilated Odin/SMR N_2O is corroborated by the ozone loss estimates obtained when cross-isentropic transport is implemented using diabatic cooling rates from the SLIMCAT model.

[58] The ozone losses found in the DIAMOND model on 14 March 2005 are plotted as functions of equivalent latitude in Figure 18. Cross-isentropic transport was implemented using diabatic cooling rates from the SLIMCAT model and the four graphs describe the Arctic ozone losses on the 550 K, 500 K, 450 K, and 400 K potential temperature levels respectively. As can also be seen in Figures 14 and 15, ozone depletion is strongest in the outer regions of the vortex on the 550 K level. On the 500 K and 450 K levels ozone depletion is on the other hand contained inside the vortex with no significant ozone depletion south
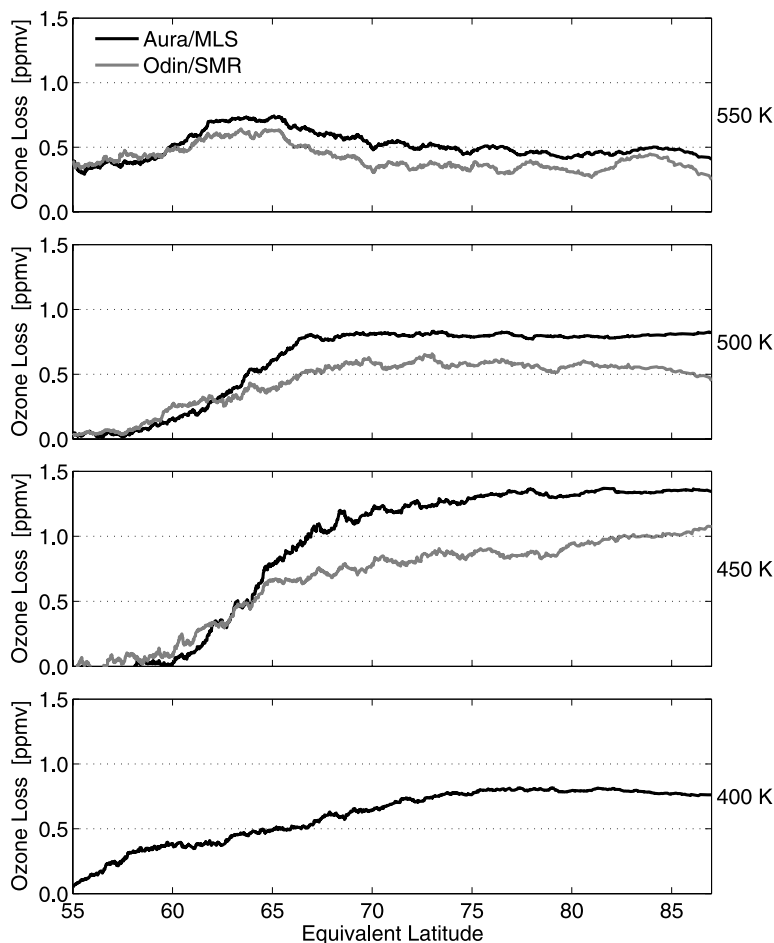
Figure 18. The four graphs describe the DIAMOND model estimates of Arctic ozone losses on 14 March 2005 as functions of equivalent latitude on the 550 K, 500 K, 450 K, and 400 K potential temperature levels.

of 60° equivalent latitude. Some ozone loss can be seen between 55° and 60° equivalent latitudes on the 400 K level since the polar vortex had already started to break up in the lowermost stratosphere.

[59] The rates of ozone depletion found north of 67° equivalent latitude in the graphs do not diverge by more than 0.2 ppmv from the respective averages north of 67°. It is therefore not possible to estimate significantly more severe average ozone depletion in the vortex by using a different equivalent latitude as definition of the vortex edge in this form of study. The choice of vortex edge definition does on the other hand matter in studies where the vortex average ozone mixing ratio in the late winter is compared directly to the vortex average ozone mixing ratio in the early winter since ozone mixing ratios are lower in the central vortex than in the outer vortex in December and early January. For example, using 60° equivalent latitude as vortex edge definition on the 550K level in the DIAMOND model on 1 January leads to 0.3 ppmv higher vortex average ozone mixing ratio than if 67° equivalent latitude is used.

8. Summary and Discussion

[60] Transport modeling of ozone fields in the 2004/2005 Arctic winter indicates splitting and other large scale dis-

ruptions of the polar vortex during February and March 2005. It is therefore likely that the expected depletion of ozone in the preprocessed vortex air was mitigated by intrusion of extravortex air masses. Instabilities during February and March furthermore lead to mixing of the ozone poor central polar vortex with the more ozone rich outer vortex regions.

[61] When interpolating Aura/MLS vortex ozone on N_2O isopleths we found 1.0−1.1 ppmv vortex average ozone depletion between 1 January and 14 March 2005 on the 100 ppbv and 150 ppbv N_2O isopleths. When interpolating Odin/SMR vortex ozone we on the other hand found 0.7− 0.9 ppmv ozone depletion on the same N_2O isopleths. On 14 March 2005, the 100 ppbv and 150 ppbv N_2O isopleths roughly correspond to the 460 K and 430 K potential temperature levels in the vortex north of 67° equivalent latitude.

[62] Assimilation of Aura/MLS ozone profiles in the DIAMOND model indicates maximum ozone loss on the 450 K potential temperature level. When cross-isentropic transport is implemented by vortex descent tuned to Aura/ MLS N_2O, we estimate 0.9 ppmv vortex average ozone depletion between 1 January to 14 March on this level. With cross-isentropic transport implemented using diabatic cool-

Table 2. Different Estimates of Vortex-Averaged Ozone Depletion in the 2004/2005 Arctic Winter[a]

Potential Temperature	Aura/MLS	Odin/SMR	*Manney et al.* [2006]	*Jin et al.* [2006]	*Rex et al.* [2006]	*Singleton et al.* [2007]
400 K	0.7 ppmv			0.8 ppmv	1.6 ± 0.3 ppmv	1.4 ppmv
450 K	1.3 ppmv	0.9 ppmv	1.2–1.5 ppmv	2.0 ppmv	1.7 ± 0.4 ppmv	2.2 ppmv
500 K	0.8 ppmv	0.6 ppmv	1.2–1.5 ppmv	2.1 ppmv	1.1 ± 0.4 ppmv	1.8 ppmv
550 K	0.5 ppmv	0.4 ppmv		1.2 ppmv	0.6 ± 0.3 ppmv	1.3 ppmv
600 K	0.4 ppmv	0.3 ppmv		0.6 ppmv		0.6 ppmv

[a]The estimates in the Aura/MLS and Odin/SMR columns have been made by assimilating ozone profiles from the two instruments into the DIAMOND model with cross isentropic transport rates taken from SLIMCAT. The four columns to the right summarize the results presented by *Manney et al.* [2006], *Jin et al.* [2006], *Rex et al.* [2006] and *Singleton et al.* [2007].

ing rates from the SLIMCAT model we estimate on the other hand 1.3 ppmv vortex average ozone loss on the 450 K level. 1.3 ppmv vortex average ozone loss based on Aura/MLS ozone measurements is also inferred when cross-isentropic transport is implemented by vortex descent tuned to Odin/SMR N_2O which is expected since descent tuned to Odin/SMR N_2O agrees well with descent derived from SLIMCAT. See Figure 6. Assimilation of Odin/SMR data indicates on the other hand less ozone depletion. On the 450 K level we estimate 0.6 and 0.9 ppmv vortex average ozone depletion respectively when vertical transport is based on Aura/MLS N_2O or on diabatic cooling rates from the SLIMCAT model. The discrepancy between Aura/MLS and Odin/SMR estimates is likely a consequence of Odin/SMR 501.5 GHz ozone data having low measurement response in the lowermost stratosphere. Typically ~70% on the 450 K potential temperature level.

[63] More severe ozone destruction in the Arctic early spring of 2005 has been reported in previous studies [e.g., *Manney et al.*, 2006; *Jin et al.*, 2006; *Rex et al.*, 2006; *Singleton et al.*, 2007]. In Table 2, the results presented in the four studies are compared to the vortex-averaged ozone depletion estimates obtained by assimilating Aura/MLS and Odin/SMR ozone profiles in the DIAMOND model with cross-isentropic transport rates from SLIMCAT.

[64] On the basis of vortex average analysis of O_3 and N_2O data from the Earth Observation System Microwave Limb Sounder (Aura/MLS) satellite instrument, *Manney et al.* [2006] estimate 1.2–1.5 ppmv vortex-averaged ozone loss between 450 K and 500 K potential temperature, with up to ~2 ppmv loss in the outer vortex near 500 K. By comparing fields of assimilated Aura/MLS ozone to passive ozone fields in which cross-isentropic transport are implemented using diabatic cooling rates from the SLIMCAT model we estimate 0.8–1.3 ppmv vortex-averaged ozone loss between 450 K and 500 K potential temperature, (see Figure 14), which is below but not that far from the loss inferred by *Manney et al.* [2006]. We can on the other hand not confirm the ~2 ppmv loss reported in the outer vortex. The discrepancy is a consequence of *Manney et al.* [2006] assuming enhanced vertical descent in the outer vortex. When comparing assimilated Aura/MLS N_2O fields to passively transported fields where cross-isentropic transport has been implemented using constant descent rates over the entire vortex we do not observe any discrepancy between the inner and outer vortex regions which would be expected if cross-isentropic transport was enhanced in the outer regions. Furthermore, the diabatic cooling fields extracted from the SLIMCAT model do not on average have enhanced cooling in the outer region of the vortex although

the variability of the cooling rates over both time and location is stronger in the outer vortex than in the central vortex. It is on the other hand possible that intravortex mixing introduced central vortex air that is relatively poor in both ozone and N_2O into the outer vortex causing both decline of ozone and overcompensation for vertical transport in the tracer correlation study of *Manney et al.* [2006]. Similar conclusions regarding the study of *Manney et al.* [2006] are stated by *Grooß and Müller* [2007] who used the CLaMS model to simulate ozone depletion in the 2004/2005 winter. *Grooß and Müller* [2007] found 1.37 ppmv vortex average ozone depletion north of ~65° equivalent latitude on the 475 K level while enhanced ozone depletion in the vortex edge region could not be confirmed.

[65] *Jin et al.* [2006] estimate ~2.1 ppmv mixing ratio losses between 475 K and 500 K by tracer correlation analysis of data from the Fourier Transform Spectrometer (FTS) instrument on board the Atmospheric Chemistry Experiment (ACE) satellite. ACE/FTS is a solar occultation instrument that retrieves atmospheric data in different latitude bands at different times of the year. In the work by *Jin et al.* [2006], data from the period 1–7 January are compared to data from 8 to 15 March 2005. During 1–7 January the instrument made 33 observations that were all located in the 56.44–60.62° N latitude band while it made 87 observations located in the 73.87–79.78° N band during 8–15 March (ACE/SCISAT-1 Database, Occultation finding tool, available at https://database.uwaterloo.ca/occultations/distance_locations.php). The instrument thus mainly observed air masses in the ozone-rich outer vortex during 1–7 January while it observed air masses from the central as well as the outer vortex during 8–15 March. When sampling the 1–7 January ACE/FTS observation locations on the 550 K level in DIAMOND, we found ozone mixing ratios that were on average 0.7 ppmv higher than the model vortex average independent of whether Odin/SMR or Aura/MLS ozone had been assimilated. DIAMOND ozone mixing ratios at the 8–15 March ACE/FTS observation locations on the 500 K model level where on the other hand 0.1 ppmv below the vortex average mixing ratios. Around 0.8 ppmv of the total ozone decline reported by *Jin et al.* [2006] can thus be attributed to inhomogeneous distribution of ozone inside the vortex and the sampling characteristics of the ACE/FTS solar occultation instrument. In a recent study, *Manney et al.* [2007] furthermore demonstrate that the ACE/FTS sampling substantially affects the estimates of vortex descent from tracers used by *Jin et al.* [2006].

[66] *Rex et al.* [2006] estimate 1.3–1.9 ppmv vortex-averaged ozone loss on the 400 K level, 1.3–2.1 ppmv ozone loss on the 450 K level and 0.7–1.5 ppmv ozone loss

on the 500 K level between 5 January and 25 March 2005 using the Match technique [*Rex et al.*, 1999] and data from in situ sondes. *Rex et al.* [2006] also reach similar results using the vortex average descent approach [*Hoppel et al.*, 2002] with data from the SAGE III and POAM III satellite instruments. The NCAR CCM radiative scheme was used to calculate cross-isentropic transport in both forms of analysis.

[67] When assimilating Aura/MLS ozone and implementing cross-isentropic transport using diabatic cooling rates from the SLIMCAT model that uses the NCAR CCM radiative scheme in our model study we estimate 0.7, 1.3 and 0.8 ppmv vortex average ozone depletion between 1 January and 14 March on the 400 K, 450 K and 500 K potential temperature levels which is within the lower range of the *Rex et al.* [2006] ozone depletion estimates on the 450 K and 500 K levels. *Rex et al.* [2006] however estimate the total vortex ozone depletion by comparing ozone mixing ratios from 5 January to mixing ratios from 25 March when the final break up of the vortex had already started and mixing with ozone poor extra vortex air caused declining ozone mixing ratios in the vortex fragments.

[68] *Singleton et al.* [2007] estimate ozone depletion in the 2004/2005 Arctic vortex by comparing a passive ozone tracer field from the SLIMCAT chemical transport model including the NCAR CCM radiative scheme, [*Chipperfield*, 2005], to ozone measurements from the Aura/MLS instrument as well as four solar occultation instruments POAM III, SAGE III, ACE/FTS and ACE/MAESTRO. Consistent results were obtained using the five different instruments and a quantitative study using Aura/MLS data sampled like the solar occultation instruments showed that sampling differences accounted for no more than 0.2–0.3 ppmv difference in estimated loss with the loss estimates from Aura/MLS being at the smaller end of the range. This would indicate that the cause of the discrepancy between our results and the results of *Singleton et al.* [2007] is not in the measurements but must be related to differences in modeling of transport and/or chemistry.

[69] In the study of *Singleton et al.* [2007], passive transport is started on 1 December 2004 and the initial ozone tracer field is obtained by running the SLIMCAT model with full chemistry for several years up until that date. By mid-March 2005, the study indicates 1.8–2.3 ppmv vortex average ozone depletion in the 425 K to 500 K potential temperature range which agrees with the ozone loss inferred by *Jin et al.* [2006] while it is more severe than the loss inferred in the studies of *Manney et al.* [2006] and *Rex et al.* [2006].

[70] When analyzing Aura/MLS ozone data, *Singleton et al.* [2007] describe less than 0.2 ppmv ozone depletion in December on potential temperature levels between 450 K and 600 K. Only a minor part of the discrepancy between our study and *Singleton et al.* [2007] is therefore explained by the fact that passive transport is started on 1 January in our study.

[71] *Singleton et al.* [2007] define the polar vortex using the vortex determination criteria of *Harvey et al.* [2002] while we use 67° equivalent latitude. The use of slightly different definitions of the polar vortex can however not explain the discrepancy between the two studies since ozone depletion exceeding 1.4 ppmv can only be found in very small areas in the DIAMOND model while ozone depletion that exceeds 1.6 ppmv cannot be found at any location in the polar vortex. See Figures 14 and 18.

[72] The discrepancy between our study and *Singleton et al.* [2007] is smaller when diabatic cooling rates from the SLIMCAT model or cross-isentropic transport rates derived by assimilating Odin/SMR N_2O are used for vertical transport in the DIAMOND model instead of cross-isentropic transport rates derived by assimilating Aura/MLS N_2O. Nevertheless we end up with 0.5–1.0 ppmv less vortex average ozone depletion than *Singleton et al.* [2007] when assimilating Aura/MLS ozone and 0.8–1.3 ppmv less vortex average ozone depletion when assimilating Odin/ SMR ozone. A significant difference between our study and the study of *Singleton et al.* [2007] is that their passive model is initialized by modeled fields while our passive model is initialized by means of assimilation of satellite data. It is however unlikely that the ozone mixing ratios in the initial passive fields of the two studies would differ by as much as 0.5–1.0 ppmv. *Singleton et al.* [2007] analyzed the impact of initializing a transport model by running a chemistry scheme in their study and concluded that it could result in ∼0.2 ppmv overestimation of ozone loss. The causes of the rather significant discrepancy between this study and the study of *Singleton et al.* [2007] thus remain unresolved.

[73] The lack of consensus in the ozone loss estimates for the 2004–2005 Arctic winter can certainly be attributed to several different factors. Published ozone loss estimates are often difficult to compare since they reflect different estimated quantities, are based on slightly different loss periods and geographical areas (determined by the assumed vortex edge definitions), and depend also on instrumental issues such as sampling, measurement noise, and altitude dependent systematic biases in the data sets. From this study, other critical uncertainties in the estimation of ozone loss in the Arctic seem to be related to establishing correct estimates and methods for the correction for vertical subsidence as well as to difficulties of some methods (e.g., vortex average and tracer correlation methods) to assess and account for quasi-horizontal isentropic mixing, which may vary considerably from year to year. This highlights the fact that a reliable analysis of Arctic ozone loss requires an analysis depending on multiple observational data sets and analysis methods allowing to eliminate outliers and artefacts, with the data assimilation method used in this study based on global satellite observations of ozone and nitrous oxide being notably valuable for the analysis of the time dependent effects of horizontal mixing.

References

Briegleb, B. P. (1992), Delta-Eddington approximation for solar radiation in the NCAR Community Climate Model, *J. Geophys. Res.*, *97*, 7603–7612.

Chipperfield, M. P. (2005), New version of the TOMCAT/SLIMCAT off-line chemical transport model: Intercomparison of stratospheric tracer experiments, *Q. J. R. Meteorol. Soc.*, *132*, 1179–1203.

Dessler, A. (2000), *The Chemistry and Physics of Stratospheric Ozone*, Elsevier, New York.

European Ozone Research Coordinating Unit (2005), The Northern Hemisphere stratosphere in the 2004/2005 winter, report, Dep. of Chem., Univ. of Cambridge, U. K.

Fahey, D. W., and A. R. Ravishankara (1999), Summer in the stratosphere, *Science*, *285*, 2008–2010.

Feng, W., et al. (2005), Three-dimensional model study of the Arctic ozone loss in 2002/03 and comparison with 1999/2000 and 2003/04, *Atmos. Chem. Phys.*, *5*, 139–152.

Feng, W., et al. (2007), Large chemical ozone loss in the 2004/2005 Arctic winter/spring, *Geophys. Res. Lett.*, *34*, L09803, doi:10.1029/2006GL029098.

Frisk, U. (2003), The Odin Satellite: I. Radiometer design and test, *Astron. Astrophys.*, *402*(3), 27–34.

Froidevaux, L., et al. (2006), Early validation analyses of atmospheric profiles from EOS MLS on the Aura satellite, *IEEE Trans. Geosci. Remote Sens.*, *44*, 1106–1121.

Grooß, J.-U., and R. Müller (2007), Simulation of ozone loss in Arctic winter 2004/2005, *Geophys. Res. Lett.*, *34*, L05804, doi:10.1029/2006GL028901.

Harvey, V. L., et al. (2002), A climatology of stratospheric polar vortices and anticyclones, *J. Geophys. Res.*, *107*(D20), 4442, doi:10.1029/2001JD001471.

Hoppel, K., et al. (2002), POAM III observations of arctic ozone loss for the 1999/2000 winter, *J. Geophys. Res.*, *107*(D20), 8262, doi:10.1029/2001JD000476.

Jin, J. J., et al. (2006), Severe Arctic ozone loss in the winter 2004/2005: Observations from ACE-FTS, *Geophys. Res. Lett.*, *33*, L15801, doi:10.1029/2006GL026752.

Jones, A. K., et al. (2007), Intercomparison of Odin/SMR Ozone measurements with MIPAS and balloonsonde data, *Can. J. Phys.*, *85*, 1111–1123.

Komhyr, W. D., T. B. Harris (1971), Development of the ECC ozonesonde, *NOAA Tech. Rep. ERL200-APCL 18*, Environmen. Res. Lab., NOAA, U. S. Dep. of Commer., Boulder, Colo.

Lambert, A., et al. (2007), Validation of the Aura Microwave Limb Sounder middle atmosphere water vapor and nitrous oxide measurements, *J. Geophys. Res.*, *112*, D24S36, doi:10.1029/2007JD008724.

Livesey, N. J. et al. (2005), EOS MLS version 1.5 level 2 data quality and description document, *JPL Doc. D-32381*, Jet Propul. Lab., Pasadena, Calif.

Livesey, N. J., et al. (2006), Retrieval algorithms for the EOS Microwave Limb Sounder (MLS), *IEEE Trans. Geosci. Remote Sens.*, *44*, 1144–1155.

Manney, G. L., et al. (2006), EOS MLS observations of ozone loss in the 2004–2005 Arctic winter, *Geophys. Res. Lett.*, *33*, L04802, doi:10.1029/2005GL024494.

Manney, G. L., et al. (2007), Solar occultation satellite data and derived meteorological products: Sampling issues and comparisons with Aura Microwave Limb Sounder, *J. Geophys. Res.*, *112*, D24S50, doi:10.1029/2007JD008709.

Müller, R., S. Tilmes, P. Konopka, J.-U. Groo, and H.-J. Jost (2005), Impact of mixing and chemical change on ozone-tracer relations in the polar vortex, *Atmos. Chem. Phys.*, *5*, 3139–3151.

Murtagh, D., et al. (2002), An overview of the Odin atmospheric mission, *Can. J. Phys.*, *80*, 309–319.

Nash, E. R., P. A. Newman, J. E. Rosenfield, and M. R. Schoeberl (1996), An objective determination of the polar vortex using Ertel's potential vorticity, *J. Geophys. Res.*, *101*, 9471–9478.

Prather, M. J. (1986), Numerical advection by conservaion of second-order moments, *J. Geophys. Res.*, *91*(D6), 6671–6681.

Rex, M., et al. (1999), Chemical ozone loss in the Arctic winter 1994/1995 as determined by the Match technique, *J. Atmos. Chem*, *32*, 35–59.

Rex, M., et al. (2006), Arctic winter 2005: Implications for stratospheric ozone loss and climate change, *Geophys. Res. Lett.*, *33*, L23808, doi:10.1029/2006GL026731.

Rösevall, J. D., et al. (2007), A study of polar ozone depletion based on sequential assimilation of satellite data from the ENVISAT/MIPAS and Odin/SMR instruments, *Atmos. Chem. Phys.*, *7*, 899–911.

Schoeberl, M., et al. (2006), Overview of the EOS Aura mission, *IEEE Trans. Geosci. Remote Sens.*, *44*, 1066–1074.

Singleton, C. S., et al. (2007), Quantifying Arctic ozone loss during the 2004–2005 winter using satellite observations and a chemical transport model, *J. Geophys. Res.*, *112*, D07304, doi:10.1029/2006JD007463.

Smit, H. G. J., and D. Kley (1996), JOSIE: The 1996 WMO international intercomparison of ozonesondes under quasi flight conditions in the environmental simulation chamber at Jülich, *Tech. Doc. 926*, World Meteorol. Organ., Geneva, Switzerland.

Tilmes, S., et al. (2004), Ozone loss and chlorine activation in the Arctic winters 1991–2003 derived with the tracer-tracer correlations, *Atmos. Chem. Phys.*, *4*, 2181–2213.

Tilmes, S., et al. (2006a), Chemical ozone loss in the Arctic and Antarctic stratosphere between 1992 and 2005, *Geophys. Res. Lett.*, *33*, L20812, doi:10.1029/2006GL026925.

Tilmes, S., et al. (2006b), Development of tracer relations and chemical ozone loss during the setup phase of the polar vortex, *J. Geophys. Res.*, *111*, D24S90, doi:10.1029/2005JD006726.

Urban, J., et al. (2006), Odin/SMR limb observations of trace gases in the polar lower stratosphere during 2004–2005, *Proceedings of the ESA Atmospheric Science Conference, 8–12 May 2006, Frascati, Italy, Eur. Space Agency Spec. Publ.*, ESA-SP-628, 5853–5870. (Available at http://earth.esrin.esa.it/workshops/atmos2006/participants/68/paper_frascati2006.pdf)

von Hobe, M., et al. (2006), Severe ozone depletion in the cold Arctic winter 2004–2005, *Geophys. Res. Lett.*, *33*, L17815, doi:10.1029/2006GL026945.

Waters, J. W., et al. (2006), The Earth Observing System Microwave Limb Sounder (EOS MLS) on the Aura satellite, *IEEE Trans. Geosci. Remote Sens.*, *44*, 1075–1092.

―――――――――――

S. Brohede, P. Eriksson, D. P. Murtagh, J. D. Rösevall, and J. Urban, Department of Radio and Space Science, Chalmers University of Technology, Hörsalsvägen 11, SE-41296 Göteborg, Sweden. (rosevall@rss.chalmers.se)

W. Feng, Institute for Atmospheric Science, School of Earth and Environment, University of Leeds, Leeds LS2 9JT, UK.